Science of the Total Environment 895 (2023) 165188

Contents lists available at ScienceDirect

Science of the Total Environment

journal homepage: www.elsevier.com/locate/scitotenv

Bio-physical determinants of sediment accumulation on an offshore coral reef: A snapshot study

Sterling B. Tebbett [a,*], Jodie A. Schlaefer [a,b], Casey L. Bowden [a], William P. Collins [a], Christopher R. Hemingson [a,c], Scott D. Ling [d], Juliano Morais [a], Renato A. Morais [a,e], Alexandre C. Siqueira [a], Robert P. Streit [a], Sam Swan [a], David R. Bellwood [a]

[a] Research Hub for Coral Reef Ecosystem Functions, College of Science and Engineering, James Cook University, Townsville, Queensland 4811, Australia
[b] Commonwealth Scientific and Industrial Research Organisation (CSIRO), Environment, Townsville, Queensland, 4811, Australia
[c] Department of Marine Science, The University of Texas at Austin, Marine Science Institute, Port Aransas, TX, USA
[d] Institute for Marine and Antarctic Studies, University of Tasmania, Hobart 7001, Australia
[e] Paris Sciences et Lettres Université, École Pratique des Hautes Études, EPHE-UPVD-CNRS, USR 3278 CRIOBE, University of Perpignan, Perpignan, France

HIGHLIGHTS

- Sedimentary process and bio-physical drivers across a reef profile were examined.
- Data were collected from the Biosphere, Hydrosphere, and Lithosphere.
- Sediment trap data did not align with patterns of on-reef sediment accumulation.
- Sediment accumulation in turfs was related to wave energy and reef geomorphology.
- Some contexts may predispose reefs to high-load turf sediment regimes.

GRAPHICAL ABSTRACT

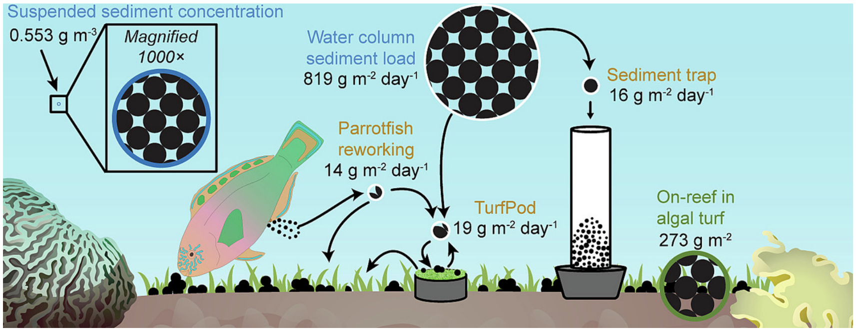

ARTICLE INFO

Editor: Filip M.G.Tack

Keywords:
Algal turf
Geo-ecological function
Parrotfish sediment reworking
Sedimentation
Sediment trap
Turbidity

ABSTRACT

Sediments are found on all coral reefs around the globe. However, the amount of sediment in different reservoirs, and the rates at which sediments move between reservoirs, can shape the biological functioning of coral reefs. Unfortunately, relatively few studies have examined reef sediment dynamics, and associated bio-physical drivers, simultaneously over matching spatial and temporal scales. This has led to a partial understanding of how sediments and living reef systems are connected, especially on clear-water offshore reefs. To address this problem, four sediment reservoirs/sedimentary processes and three bio-physical drivers were quantified across seven different reef habitats/depths at Lizard Island, an exposed mid-shelf reef on the Great Barrier Reef. Even in this clear-water reef location a substantial load of suspended sediment passed over the reef; a load theoretically capable of replacing the entire standing stock of on-reef turf sediments in just 8 h. However, quantification of actual sediment deposition suggested that just 2 % of this passing sediment settled on the reef. The data also revealed marked spatial incongruence in sediment deposition (sediment trap data) and accumulation (TurfPod data) across the reef profile, with the flat and back reef emerging as key areas of both deposition and accumulation. By contrast, the shallow windward reef crest was an area of deposition but had a limited capacity for sediment accumulation. These cross-reef patterns related to wave energy and reef geomorphology, with low sediment accumulation on the ecologically important reef crest aligning with substantial wave energy. These findings reveal a disconnect between patterns of sediment deposition and accumulation on the benthos, with the 'post-settlement' fate of sediments dependent on local hydrodynamic conditions. From

---

* Corresponding author.
E-mail address: sterling.tebbett@my.jcu.edu.au (S.B. Tebbett).

http://dx.doi.org/10.1016/j.scitotenv.2023.165188
Received 18 April 2023; Received in revised form 15 June 2023; Accepted 26 June 2023

an ecological perspective, the data suggests key contextual constraints (wave energy and reef geomorphology) may predispose some reefs or reef areas to high-load turf sediment regimes.

1. Introduction

As coral reefs rapidly degrade in the Anthropocene, understanding the range of stressors that act on these ecosystems is critical (Harborne et al., 2017; Hughes et al., 2017). In this respect, declining water quality and increased sediment inputs to reefs represent a major stressor with the potential to vary considerably under different contexts (Bainbridge et al., 2018; Suárez-Castro et al., 2021; Andrello et al., 2022). This is because sediments are shaped by a complex suite of processes which operate and interact on, in, and around reefs. Sediment distributions can be influenced by physical factors such as currents and waves (Wolanski et al., 2003; Ogston et al., 2004; Storlazzi et al., 2004; Browne et al., 2013a; Cartwright et al., 2021), and reef geomorphology (Golbuu et al., 2003, 2011; Kench and Brander, 2006), as well as biological drivers such as the feeding activity of fishes (Bellwood, 1996; Bowden et al., 2022; Perry et al., 2022) and the type of benthic biota (Reeves et al., 2018; Pessarrodona et al., 2021). This complex array of factors leads to marked variability in the amount and type of sediment in different coral reef reservoirs (e.g. the water column, on-reef surfaces, and off-reef sediment aprons) (Storlazzi and Jaffe, 2008; Harris et al., 2014; Tebbett et al., 2017a). These factors also determine the extent to which sediments move between coral reef reservoirs (e.g. sedimentation and resuspension) (Orpin et al., 1999; Storlazzi et al., 2009; Browne et al., 2013a; Whinney et al., 2017). It is this complexity, perhaps, that has resulted in different sediment reservoirs, and their associated linking processes, being largely studied in isolation (reviewed in Schlaefer et al., 2021).

Studies where multiple sediment reservoirs and linking processes have been measured simultaneously are rare. However, those that do exist have provided valuable insights into sediment dynamics on, in and around coral reefs (e.g. Wolanski et al., 2005; Storlazzi et al., 2009; Whinney et al., 2017; Schlaefer et al., 2022). For example, a recent study from Orpheus Island, an inshore coral reef on Australia's Great Barrier Reef (GBR), quantified multiple sediment reservoirs and linking processes across a coral reef depth gradient (Schlaefer et al., 2022). In doing so, this study revealed a marked potential for the water column to deliver sediments to the reef, and supported the existence of two different sediment regimes (high dynamic vs. low dynamic) across coral reef depth/habitat gradients (Schlaefer et al., 2022; also see Wolanski et al., 2005). Nevertheless, this previous study was limited to a single sheltered location on an inshore reef. As such, the generality of these insights to other coral reef systems remains unclear.

Beyond cross-depth gradients, major axes of variation in coral reef functioning exist across exposure regimes (Bejarano et al., 2017; Taylor et al., 2018; Roff et al., 2019) and cross-shelf gradients (i.e. distance from land) (Cleary et al., 2016; Ryan et al., 2018; McClure et al., 2019; Moustaka et al., 2019). Sediment dynamics are one example of the processes that are known to vary substantially across these gradients. For example, the loads of sediments in the water column (i.e. turbidity) generally decrease with distance from land (Weeks et al., 2012; Fabricius et al., 2014) and heavy wave action on exposed windward reef crests may limit sediment accumulation on surfaces (Purcell, 2000). This variation in sediments has been linked to a range of critical ecosystem processes such as herbivory (Albert et al., 2008; Goatley and Bellwood, 2012; Duran et al., 2019) and coral settlement (Evans et al., 2020; Ricardo et al., 2021; Doropoulos et al., 2022) and can thus directly shape how a given reef functions. However, despite the important role of sediments in structuring ecosystem processes, we have a surprisingly limited understanding of how sediments, and the complex suites of drivers that structure their distributions, operate on clear-water, exposed, windward reefs when compared to their turbid-water counterparts.

Given the ubiquity of sediments on reefs and their interaction with critical ecosystem processes, a better understanding of the links between different sediment reservoirs and the relative importance of different bio-physical drivers is needed. This is particularly true for exposed offshore reefs, in which detailed quantification of reef processes can be particularly challenging. To address this issue, the aim of this study was to comprehensively, and simultaneously, quantify numerous components of sediment dynamics on a windward, mid-shelf reef on the GBR. Specifically, we quantified four sediment reservoirs/sedimentary processes (i.e. suspended sediments, sediment trapping rates, sediment accumulation on TurfPods, and sediment standing stock in algal turfs) and three bio-physical drivers (i.e. wave energy, current speed, and parrotfish sediment reworking) over six days across seven different habitats/depths on an exposed, windward mid-shelf reef at Lizard Island. As a result, this study will permit comprehensive insights into the relative importance of different bio-physical drivers in structuring sediments on a windward, offshore coral reef.

2. Methods

2.1. Study site

Data were collected at Lizard Island in the northern Great Barrier Reef (GBR) (Fig. 1). Lizard Island is located approximately 30 km from the mainland, outside of the inner-shelf sediment wedge on the GBR (Larcombe and Woolfe, 1999), with minimal exposure to terrestrial sediment inputs (Fabricius et al., 2016). At this location, we established a study site on a windward section of reef between Bird and South Island, that is exposed to the regular SE trade winds and has a typical cross-reef profile (Fig. 1). Sampling at Lizard Island was undertaken over six days from the 27th of January until the 2nd of February 2021 during the monsoon season. The tidal and wind conditions during the study period were relatively typical. That is, the tidal range during sampling (0.6–2.4 m) captured the interquartile range and the upper extreme (Fig. S1), while the winds were predominantly from the south-southeast/southeast/east-southeast and had speeds of 4.5–12 m s^{-1} (Fig. S2). Such winds occur on approximately 91 % of the days in the trade wind season and 54 % of the days in the monsoon season (Fig. S2).

At the study site, three transects were established to ensure a broad section of the reef was sampled (Figs. 1, S3). The three transects were ~ 25 m apart and established parallel to each other across the reef profile from the back reef, across the flat to the outer-reef flat/crest at 3 m and then down to 12 m on the reef slope (with all depths cited hereafter referring to the maximum depth during the study period unless otherwise stated). Along each transect, seven discrete habitat/depths were sampled (back reef, mid-flat, 3, 4.5, 6, 9, and 12 m). It is important to note that all complementary components of the study were collected within this delineated area, however, intensive sampling of sediments and all bio-physical drivers focused on the five depths (i.e. from 3 to 12 m), which is termed the 'reef section' hereafter. Additional sampling on the mid-flat and back reef were conducted to provide further insights into sediment dynamics across the entire reef profile. The 'sediments' considered here included both inorganic and organic particulate material <2 mm in diameter (sands, silts and clays: ISO 14688-1:2017). Below we first focus on the measurement of values pertaining to the entire 'reef section' scale, and then at the 'across depth/habitat' scale. Sampling methods follow those of Schlaefer et al. (2022) and are outlined below.

2.2. Total reef section sediment dynamics

2.2.1. Overview

At the total reef section scale, we simultaneously examined the potential supply of sediment from the water column sediment reservoir, the potential supply from sediment reworking by parrotfishes, and benthic sediment

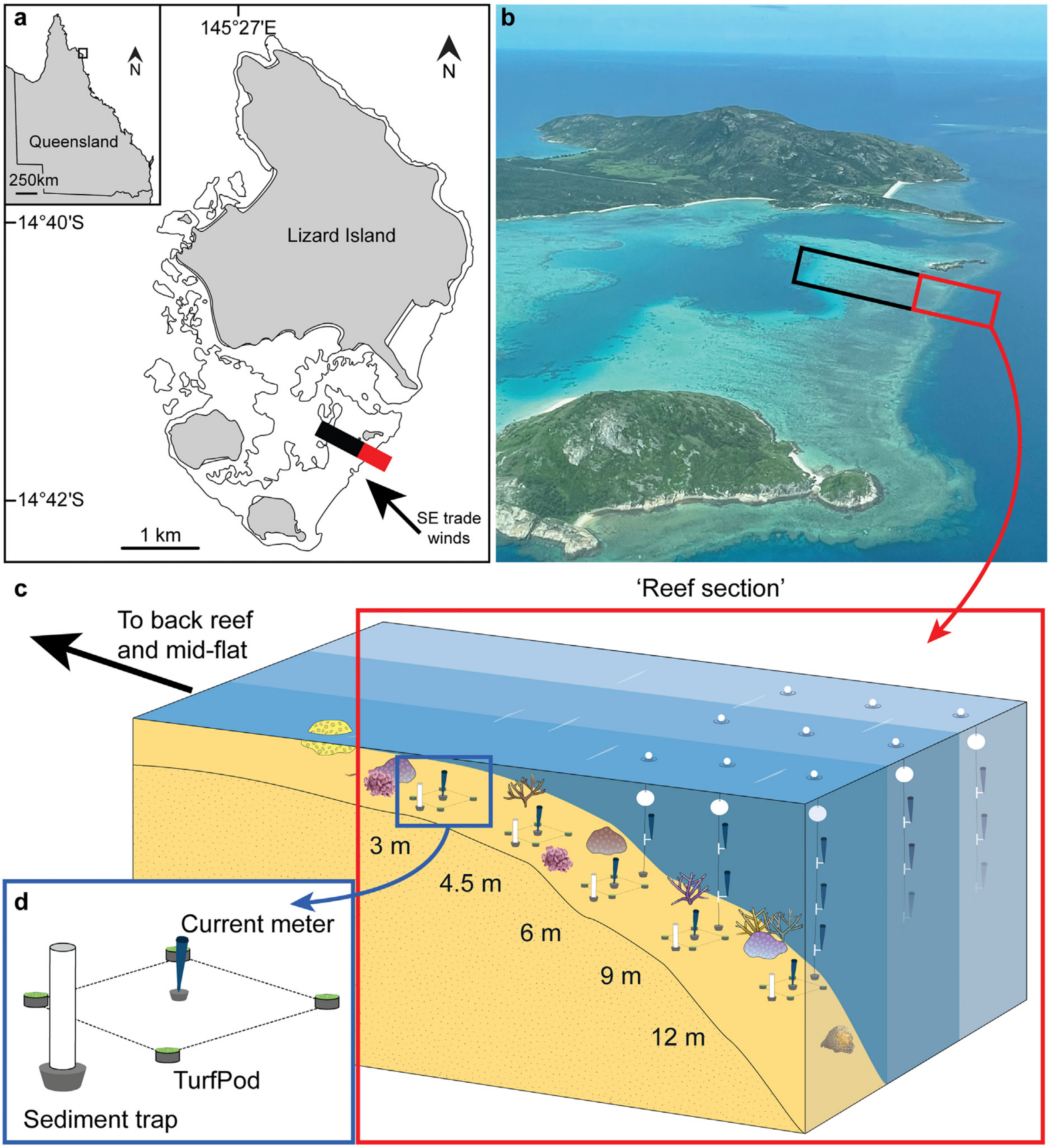

Fig. 1. Study location and sampling design. a) The location of the study area (black and red boxes) at Lizard Island. Note that the red box denotes the main sampling 'reef section' while the black box shows the rest of the cross-reef profile sampled. The inset shows the location of Lizard Island relative to Queensland, Australia. b) Photograph of the Lizard Island reef complex showing the main study area (denoted by the black/red boxes). c) Diagrammatic representation of the sediment sampling array showing sampling at each depth (3, 4.5, 6, 9, and 12 m). The diagram shows bottom-deployed and on-line current meters, as well as sediment traps and TurfPods. Note that the equipment deployed on the bottom is only visualised for one of the three transects. d) Shows an enlarged version of the benthic sampling array for clarity.

deposition and accumulation rates. The magnitudes of sediment supply and delivery were then placed into perspective based on the standing stock of sediments contained on the benthos in natural turfs. Each of the four key components pertaining to sediment supply are outlined below, while details of how algal turf sediment standing stock was measured are outlined in Text S1.

2.2.2. The water column sediment reservoir

The mass of sediment suspended in the water column that travelled through the reef section during the six-day study period was calculated to examine the potential for the water column to supply sediments to the reef. To do this, we combined estimates of the average suspended sediment concentration and the volume of water travelling through the reef section during the study period. The suspended sediment concentration was estimated from extensive turbidity profiling. The profiling was conducted over 6 days at Lizard Island, from 28th January to 3rd February 2021, and one flood and one ebb tide were profiled per day. On each tide, three turbidity profiles were measured from the water column directly in front of the reef section, at the 18, 21 and 24 m depth contours (Seapoint Tu sensor with sampling frequency = 3; Fig. S3); therefore, 36 profiles were measured in total. The profiles were taken in front of the reef section instead of adjacent to it as the wave activity made it too dangerous to measure the turbidity over the reef. The average turbidity over the top 12 m of the water column (maximum reef section depth) was calculated from turbidity profiles, and then a standard conversion factor (1.33; following previous studies on the GBR [Devlin and Schaffelke, 2009;

Davidson et al., 2019]) was applied to convert the turbidity (Nephelometric Turbidity Units, NTU) to an estimated suspended sediment concentration (g m^{-3}; Fig. S4). It is important to note that this conversion factor can be context dependent, although the value we used was based on sampling of multiple reefs on the GBR (Schaffelke et al., 2009) and is comparable to conversion factors derived for other locations (Larcombe et al., 1995; Jones et al., 2015; Cartwright et al., 2022).

The volume of water travelling through the reef section was quantified based on depth-stratified current data. Currents were measured using an array of 33 Marrotte HS drag-tilt current meters. For this analysis, we used the current meters on the boundary transects of the reef section (i.e. not the middle transect) as well as at the shallowest and deepest sites of the middle transect (i.e. 30 current meters out of the 33 deployed), to quantify the fluxes of water volume across the reef section boundary. Current meters were deployed on the benthos using two dive weights each, at each of the five depths (3, 4.5, 6, 9, and 12 m) in each of the three reef profile transects (Fig. 1). In addition, at sites with depths of 6 m or more, currents in the water column were measured using meters deployed on taut rope lines. To hold the lines taut, we utilised heavy concrete blocks (3 × 10 kg blocks with an effective mass of ~17 kg in seawater) and two spherical polystyrene sub-surface buoys (20 cm and 15 cm in diameter providing approximately 6 kg of buoyancy/tension). This provided a firm point of attachment for the current meters (see Schlaefer et al., 2022 for a comprehensive overview of the accuracy of this method). To attach meters to the taut rope lines, we used horizontal 30 cm sections of PVC pipe to hold the current meters off the line and ensure the rope could not interfere with the meters. Current meters were attached to ropes at 3 m intervals (starting and ending 3 m above/below the benthos/water surface, respectively) with 1, 2 and 3 current meters attached to ropes moored at depths of 6, 9 and 12 m respectively. Thereby, the boundary sites had a subset of 27 of the 33 current meters in the array. The placement of the meters ensured that they were always submerged by at least 0.6 m of water given the maximum tidal range during the study period (2.4 m), minimising the interference of high-frequency orbital wave velocities (which are strongest in surface waters [Soulsby et al., 1993]). The influence of orbital waves was further factored-out by averaging the high-frequency (1 measurement per second) raw current measurements to a lower frequency (10 min) during post-processing of the data. Based on a rigorous data quality control procedure (see Text S2) it was necessary to exclude data from 3 of the 27 current meters.

Ultimately, the potential sediment supply from the water column to the reef was calculated by multiplying the average suspended sediment concentration by the water volume that travelled through the reef section. For this calculation, the sites on the boundary of the reef section formed 11 vertical faces of an irregular prism (Fig. S3). The depth stratified water current velocity (m s^{-1}) that was orientated perpendicular to each of the prism faces was calculated from the current measurements at the edge sites, and then linearly interpolated onto a fixed grid with 0.25 m resolution. The grid length was equal to the distance between edges, while the grid depth equalled the average depth of the deeper of the two edge sites. Multiplying the perpendicular speed component by the cell area (m^2) yielded the instantaneous volumetric flow (m^3 s^{-1}). Multiplying this value by the average suspended sediment concentration (g m^{-3}), and the time bin interval (10 min) resulted in the cell-level sediment mass flow over each time bin (g). The cell-level masses were then summed across all cells and prism faces, as well as balanced through time, to yield an estimate of the total mass of sediment travelling over the reef section in the 6-day study period.

2.2.3. Parrotfish sediment reworking

Given the substantial role of parrotfishes in reworking sediments (Bellwood, 1996; Perry et al., 2022), we estimated the potential magnitude of their contribution to this geo-ecological function. To do this, we used a two-step, depth stratified underwater visual census and combined this with sediment reworking rate data from the literature. Specifically, at each of the five depths (i.e. 3, 4.5, 6, 9, and 12 m), parrotfishes (as well as rabbitfishes and surgeonfishes) were counted along a 50 m-long transect. Transects were parallel to one another, perpendicular to the reef profile, and consecutive transects were typically located >10 m apart to minimise the probability of counting the same fish twice. First, all fishes >10 cm total length (TL), within a 5 m belt, were surveyed as the transect tape was laid. On the return pass all individuals <10 cm TL were surveyed within a 1 m belt. Relevant fishes were identified to species, counted and their size was estimated (to the nearest 2 cm for individuals <30 cm and to the nearest 5 cm for individuals >30 cm). Combined, the census covered a total area of 1250 m^2 or approximately 100 % of the whole reef section.

Based on the visual census data, we estimated parrotfish sediment reworking following Hoey and Bellwood (2008) using the formula:

$$\mathrm{Rw_d} = \sum_{i=1}^{n} \left(\mathrm{F_{id} L_{id} B_{id} S_d}\right) \times \frac{1}{1000}$$

where the depth-specific (*d*) reworking rate Rw_d (g m^{-2} day^{-1}) of the number of individual (*n*) parrotfishes was the result of summing the products of their individual (*i*) feeding rates F_{id} (bites min^{-1}), feeding day lengths L_{id} (min) and bite areas B_{id} (mm^2 $bite^{-1}$), multiplied by the depth-specific standing stock sediment load S_d (g mm^{-2}). Average values for each of the parrotfish parameters were sourced from previous studies on the GBR. Feeding rate data were obtained from Bellwood and Choat (1990) and Bonaldo and Bellwood (2008) and were entered as species-level averages for the 11 species recorded (*Cetoscarus ocellatus*, *Chlorurus bleekeri*, *C. microrhinos*, *C. spilurus*, *Scarus chameleon*, *S. flavipectoralis*, *S. frenatus*, *S. niger*, *S. psittacus*, *S. rivulatus*, *S. schlegeli*). Day length was considered the period between sunrise and sunset during the study period and was obtained from the package *geosphere* in R (Hijmans, 2022). Variation in the diel rate of parrotfish feeding was also accounted for using data sourced from Bonaldo and Bellwood (2008) to determine the daily cumulative proportion of mean bite rate at different periods throughout the day. Parrotfish bite area was modelled separately for *C. ocellatus*, *Chlorurus* spp. and *Scarus* spp. as a function of body length in a gamma distributed (log-link) generalised linear model. Specifically, we used size and species-specific data (sourced from Bonaldo and Bellwood, 2008; Hoey, 2018) as inputs and linearly interpolated predictions for each individual. Finally, the standing stock of sediments in the algal turfs available for re-working was based on samples collected in the study location (see Text S1 for quantification details).

2.2.4. Sediment deposition/accumulation

The potential capacity for the water column to supply sediments to the reef (see above) was compared to the realised delivery of sediments to the reef based on two proxies for benthic sediment deposition/accumulation, at each depth along each reef profile transect. At each sampling area, four TurfPods deployed on the bottom delineated a 4 m^2 square, while the current meters denoted the centre (Fig. 1d). These TurfPods were concrete-filled PVC bases (7 cm high, 9 cm diameter), with 7 mm long artificial plastic grass attached (see Latrille et al., 2019 for details). These TurfPods were secured to the substratum (Table S1) and acted as a proxy for sediment accumulation in algal turfs. We focused on algal turfs because they are the predominant benthic covering at Lizard Island (Tebbett et al., 2022a) as well as on most coral reefs globally (Smith et al., 2016; Jouffray et al., 2019; Tebbett et al., 2023a), and are poised to dominate on future reef systems (Agostini et al., 2021; Harvey et al., 2021). Importantly, TurfPods quantify net sediment accumulation rather than a gross 'trapping rate' as they allow for both sedimentation, accumulation, and resuspension (Latrille et al., 2019). 'Trapping rate' (i.e. gross sediment deposition from the water column) was estimated separately, using sediment traps constructed from 60 cm long, 9 cm diameter PVC pipes set into concrete bases. One trap was deployed immediately adjacent to each of the 4 m^2 square sampling areas (Fig. 1d). Such traps do not allow resuspension of collected sediments, and due to their elevation 60 cm above the substratum, they quantify potential water column supply of sediments more so than near-bed (i.e. <30 cm) sediment resuspension and deposition (Bothner et al., 2006; Storlazzi et al., 2011; Ng et al., 2022). TurfPods and sediment traps were all deployed on the same day at the start of sampling and collected on the same day at the end of sampling (see Table S2 for the final number of replicates for each method at each depth) with collection methods following Latrille et al. (2019). A decanting, sieving, drying, and weighing procedure was used to determine the mass of sediments accumulated on TurfPods and in sediment traps (see Text S1 for full details).

2.3. Across-depth/habitat sediment dynamics

In addition to exploring sediment dynamics at the scale of the total reef section, we also examined how sediment dynamics varied across the depth/habitat gradient. At each sampling depth of 3, 4.5, 6, 9, and 12 m, we simultaneously collected data on: a) benthic sediment deposition/accumulation, b) sediment reworking by parrotfishes, c) near-bottom currents, and d) the propensity for wave-driven sediment resuspension. In addition, at the mid-flat and back reef sampling areas we collected data on benthic sediment deposition/accumulation. Methods for sediment deposition/accumulation and parrotfish sediment reworking are outlined above, while details pertaining to the depth-specific quantification of currents and wave energy are detailed below.

To examine near-bottom current-driven water movement, we used data collected from the current meters deployed on the bottom in the centre of each of the 4 m^2 sampling areas ($n = 13$ current meters, as 2 of the 15 on-bottom current meters were excluded following the data quality control procedure [see Text S2]). As currents can resuspend sediments by exerting shear stress on the benthos (Grant and Madsen, 1979; Soulsby et al., 1993), we examined variability in current speed across the different depths. Current data were processed as described above. To examine the potential for wave energy to resuspend sediments across the depth gradient, we utilised data derived from 3 pressure sensors (RBRsolo3) deployed along the middle transect at 3, 6, and 12 m. The pressure sensors were securely mounted on hard substrata and programmed to record 16 measurements per second to capture the high-frequency change in pressure exerted on the bottom by waves. To isolate high-frequency wave-driven changes from low-frequency tide-driven changes we used a rolling analysis with a 5-min time step. Wave-driven pressure change was subsequently calculated based on the average absolute high-frequency pressure residual around the linear regression line denoting the tide-associated low-frequency pressure change (using python 3 package: statsmodel 0.12.2; Seabold and Perktold, 2010). Importantly, we directly analysed bottom pressure measurements (i.e. from the location of resuspension) and, therefore, we did not derive secondary products from the pressure data (e.g. bed shear stress or wave orbital velocities) as this would have introduced unnecessary complexities, assumptions and associated uncertainty. As resuspension of sediments occurs when the stress exerted on the bottom by waves and/or currents exceeds a threshold (Jing and Ridd, 1996), we plotted the distribution, rather than averages, for the cross-depth hydrodynamic data. To gain an insight into maximum wave energy across the entire reef profile, we also re-deployed three RBRsolo3 pressure sensors between the 18th and 23rd of February 2021 on the back reef, crest, and slope (at 12 m).

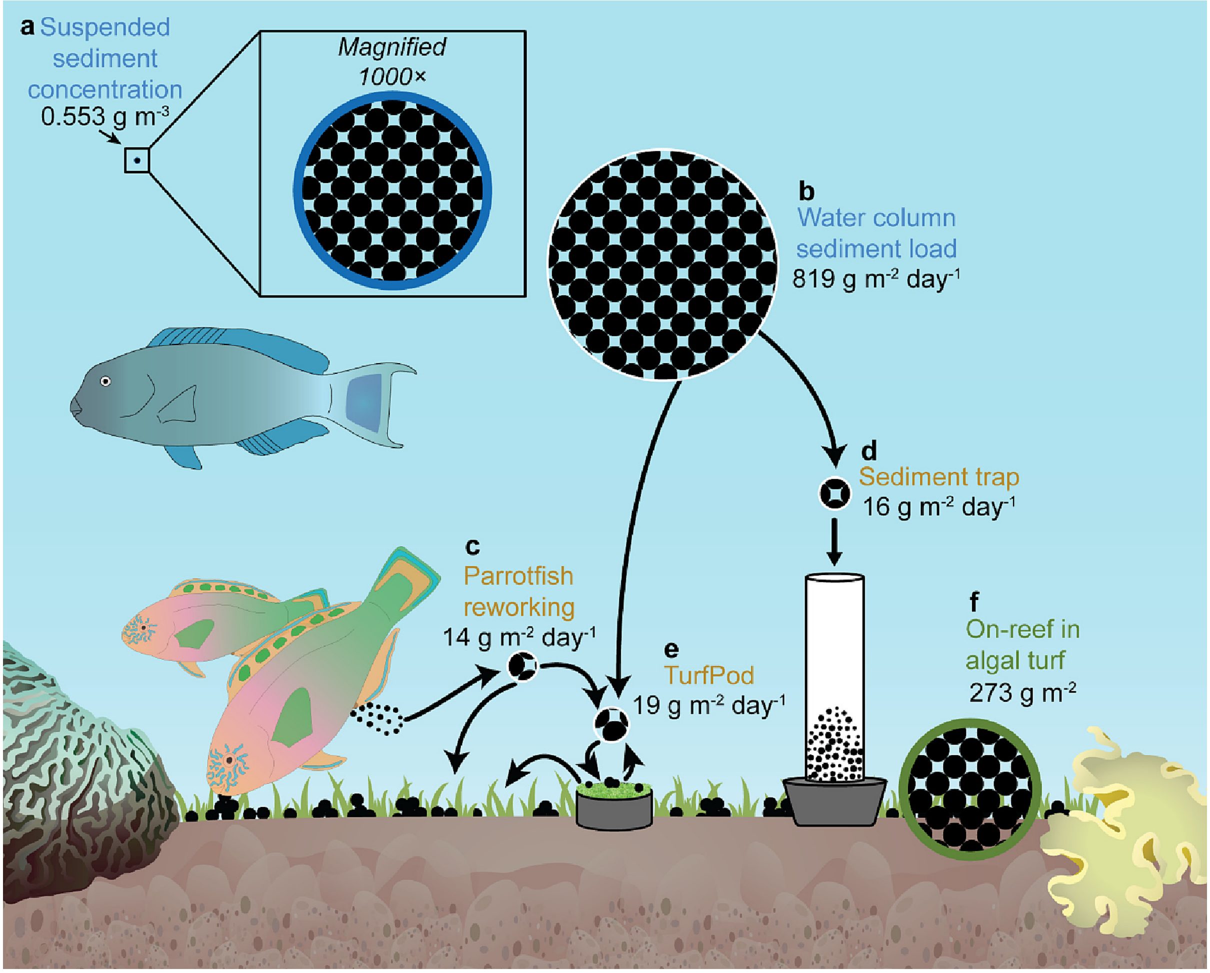

Fig. 2. Total reef section sediment dynamics at Lizard Island. The point clouds enclosed by white circles represent daily rates, while the point clouds enclosed by blue/green circles represent a standing stock reservoir (i.e. sediment standing stock in the water column [blue] and in turfs [green]). Note the area of the point clouds is scaled to the magnitude of the rate/standing stock. The black arrows show the direction of sediment movement. The stocks/rates measured were a) the standing stock of sediment in the water column, b) the amount of sediment in the water column that moved through the array site, c) sediment reworked by parrotfishes, d) sediment accumulation in traps, e) sediment accumulation on TurfPods and f) the standing stock of sediment on the reef in algal turfs.

2.4. Statistical analyses

Initially, we examined sediment dynamics across the entire cross-reef profile (i.e. from 12 m on the reef slope across to the back reef) at Lizard Island. Specifically, we examined how algal turf sediment loads ($n = 10$ samples in each habitat: back, mid-flat, crest, and slope) differed among habitats using a generalised linear model (GLM) with a Gamma distribution and log-link function. In this case, habitat/depth was treated as a categorical fixed effect. In addition, we examined how sediment accumulation on TurfPods ($n =$ 2–4 at each sampling square as some replicates were lost due to dislodgement [Table S2]) varied among the seven habitats/depths sampled using a generalised linear mixed-effects model (GLMM). Again, this model was based on a Gamma distribution and log-link function and incorporated habitat/depth as a fixed effect. However, this model also incorporated transect site as a random effect to account for any spatial lack of independence. In both cases, post-hoc pairwise means comparisons were performed with a Tukey's adjustment to examine within factor differences. Model fit and assumptions were examined via residuals using simulation-based model-checking, which suggested model fit was satisfactory in all cases. Due to the loss of some sediment trap replicates (n = 1–3 at each depth [Table S2]), and the need to treat habitat/depth as categorical factor in these analyses, we explored cross-reef patterns of sediment trap data graphically.

Following examination at the entire cross-reef profile scale, we focused in on the ‘reef section’ (i.e. 3–12 m) where detailed quantification of bio-physical drivers occurred. Accumulated sediment mass was treated as the response variable in respective generalised linear mixed effects models (GLMMs) for the TurfPod and sediment trap data. Both models were based on Gamma distributions with a log-link function. As there were no ‘habitat’ levels in this reef section data, depth (3–12 m) in this case was treated as a continuous fixed effect to examine general trends. Transect site was again treated as a random effect to account for any lack of spatial independence. Data exploration suggested some degree of non-linearity across depth, and this was accounted for by modelling depth using a third order polynomial in both cases. All model fit and assumptions were examined via residuals using simulation-based model-checking (Hartig, 2020), which suggested model fit was satisfactory in all cases. All statistical analyses and plotting was performed in the software R (R Core Team, 2022) using the *glmmTMB* (Brooks et al., 2017), DHARMa (Hartig, 2020), and *emmeans* (Lenth, 2020) packages.

3. Results

3.1. Total reef section sediment standing stocks and fluxes

During the study period, the average suspended sediment concentration (i.e. water column standing stock) was 0.553 g m^{-3} (Fig. 2), with little variation in turbidity across depths (Fig. S4). By contrast, the average standing stock of sediment bound in the turfs at the study site was 273 g m^{-2} (Fig. 2). Therefore, based on a single frame in time, there was ~494-fold more sediment bound in the turf than in the water column on a m^2 versus m^3 basis. However, by combining the suspended sediment concentration with the estimate of total water volume that moved over the reef section during the study period (10,894,603 m^3), we estimated that a total of 6.0 ± 0.1 t of sediment moved over the site during the 6-day period. This equates to 819 g m^{-2} day^{-1} when partitioned by area (1226 m^2) and day (Fig. 2). Interestingly, this quantity of sediment moving over the study site in a day was 3-fold greater than that bound in the turfs, suggesting that if all this sediment settled out of suspension it had the capacity to replace all of the sediment trapped in turfs in just 8 h (Fig. 2).

Simultaneously examining two metrics of sediment deposition/accumulation (i.e. sediment trapping rate and sediment accumulation on TurfPods) provided insights into the relative strength of connections between the water column and benthic turf sediments. Specifically, despite 819 g m^{-2} day^{-1} of sediment transiting over the site, sediment trapping rates were only 16 g m^{-2} day^{-1}, or just 2 % of the total amount of sediment that passed over the reef (Fig. 2). Overall, accumulation of sediments on TurfPods was ~1.2-fold higher than in sediment traps (Fig. 2). However, this still suggests that just 2.3 % of the sediment passing over the reef accumulated on TurfPods each day. When sediment accumulation rates on TurfPods were compared to the standing stock of sediments in natural turfs, 7 % of the standing stock was found to accumulate each day on TurfPods. Based on this rate of accumulation it would take ~14 days for the entire standing stock of turf sediments to be replaced. Finally, the parrotfish community reworked the standing stock of sediments in the turfs at a rate of 5.1 % day^{-1}.

3.2. Across-depth/habitat sediment dynamics

Sediment dynamics varied considerably across the windward reef habitat gradient examined at Lizard Island (Fig. 3a-d). Sediment standing stock, accumulation on TurfPods, and accumulation in traps were all highest in the shallow reef flat or back reef habitats when compared to the reef crest and reef slope habitats (Fig. 3b-d). In terms of sediment standing stock in algal turfs, average sediment loads were >17.4-fold higher on the flat compared to the crest (3907 vs. 224 g m^{-2}) (Fig. 3b; Table S3). Indeed, the GLM revealed that sediment loads in reef flat algal turfs were significantly higher than in all other habitats ($p < 0.05$ in all cases; Tables S3, S4). Accumulation rates in sediment traps also followed a similar trend, with the highest average (±SE) rates on the flat (322.2 ± 160 g m^{-2} day^{-1}) and the lowest at 12 m on the reef slope (9.5 ± 0.3 g m^{-2} day^{-1}) (Fig. 3d). By contrast, sediment accumulation rates on TurfPods were significantly higher in the back reef compared to all other habitats/depths sampled ($p < 0.05$ in all cases; Table S4), while accumulation rates on TurfPods on reef flat habitats were significantly higher than TurfPods at 3, 4.5, and 9 m (Table S4). The hydrodynamic forces also appeared to vary considerably across the same gradient (Fig. 3a). Specifically, wave energy on the benthos was highest on the shallow windward reef face (maximum recorded = 0.08 dbar), while dissipating across the profile in the sheltered lagoonal back reef (maximum recorded = 0.04 dbar) (Fig. 3a). These patterns suggest that hydrodynamic drivers and associated sedimentary processes, differ markedly across this windward reef profile.

When the cross-depth patterns were considered in more detail across the crest-slope reef section, marked divergences in sediment accumulation in traps versus on TurfPods were revealed (Fig. 3e). Specifically, a GLMM revealed that there was a significant third-order polynomial relationship between sediment accumulation rate on TurfPods and depth, with accumulation rates increasing from 3 m to 6 m before leveling out ($p < 0.05$; Fig. 3e; Table S5). By contrast, a GLMM revealed that there was a significant second-order polynomial relationship between sediment trapping rate and depth, with trapping rate declining markedly from 3 m to 6 m before leveling out ($p < 0.05$; Fig. 3e; Table S5). Consideration of how near-bed currents and wave pressure on the benthos varied across the same depth gradient was informative for these sediment dynamics. The speed and range of water currents near the benthos were remarkably similar across the depth gradient (Fig. 3f). By contrast, the total pressure, and range of pressures, that waves exerted on the benthos declined markedly across the depth gradient (Fig. 3g). Maximum wave pressure declined by 4.3-fold across the 3 to 12 m depth gradient (Fig. 3g). Finally, parrotfish sediment reworking rates also appeared to vary markedly across the depth gradient (Fig. 3h). Parrotfishes were estimated to rework sediments from a rate of 1.6 g m^{-2} day^{-1} at 3 m, up to 33 g m^{-2} day^{-1} at 9 m, while reworking rates at 4.5, 6 and 9 m ranged between 10.8 and 13.4 g m^{-2} day^{-1} (Fig. 3h).

4. Discussion

In this study, we quantified a suite of sedimentary processes and associated bio-physical drivers in a high-resolution snapshot of sediment dynamics across an entire reef profile in a windward, clear-water location. The data suggests that even in clear-water reef locations, a substantial load of sediment passes over the reef in the water column, with this load capable of replacing the standing stock of turf sediments in just 8 h if all sediment was deposited. However, data from both sediment traps and TurfPods

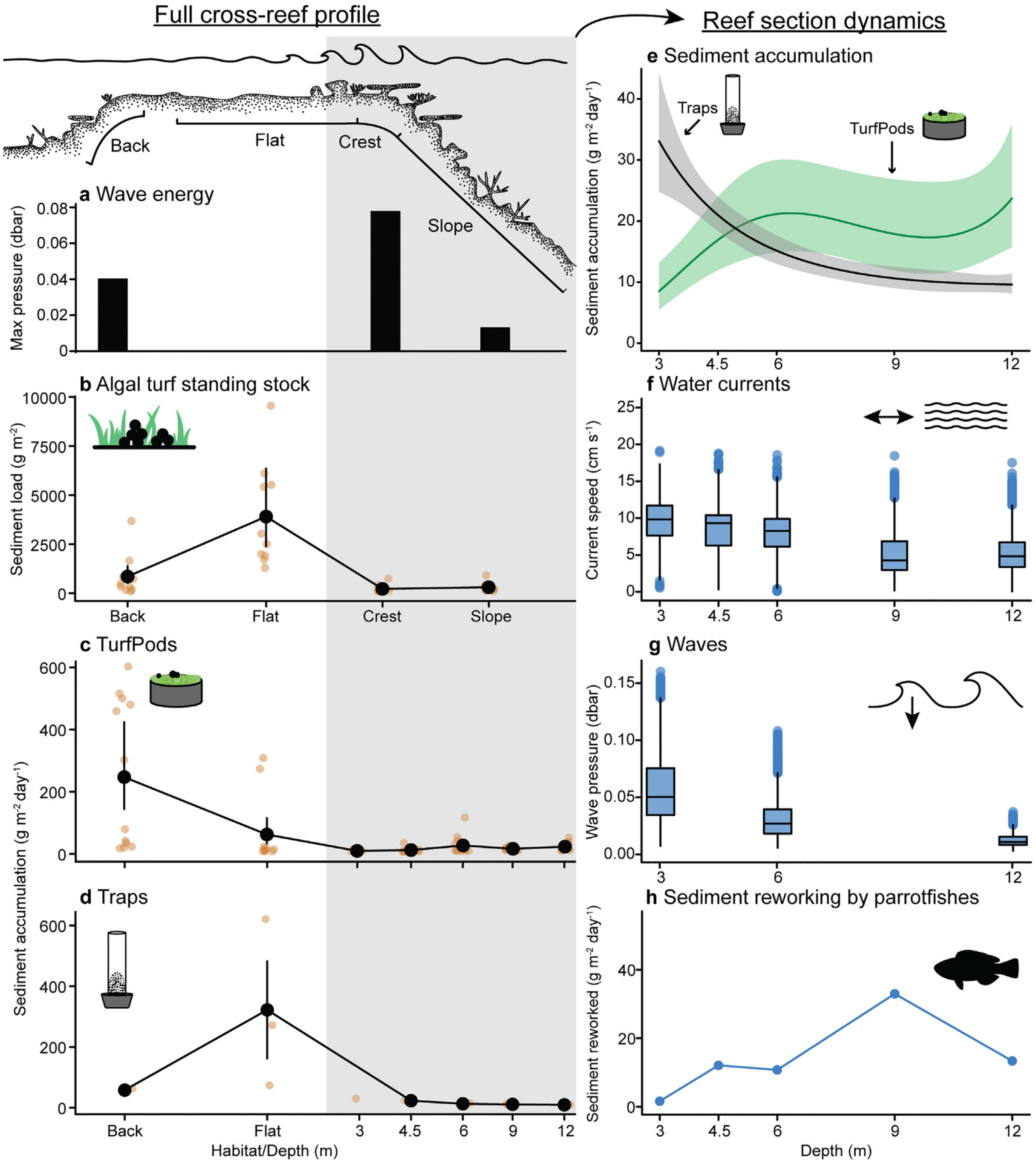

Fig. 3. Sediment dynamics across a windward coral reef profile at Lizard Island. a) Maximum wave pressure on the benthos recorded in back, crest and slope habitats between 18 and 23 February 2021. b) The standing stock of sediment loads in algal turfs across the four habitats. Accumulation rate of sediments c) on TurfPods and d) in sediment traps. The black point and ranges in b) and c) denote the mean predicted fit and 95 % confidence intervals from generalised linear/generalised linear mixed effects models. The black point and ranges in d) denote the mean (± SE) of the raw data. Pale orange points in b-d) denote the raw data points. The grey shaded box (a-d) denotes the area of the reef profile quantified in more detail (e-h). e) Variation in cross-depth sediment accumulation on TurfPods and in sediment traps (lines denote the mean predicted fit from generalised linear mixed effects models while coloured ribbons denote the 95 % confidence intervals). Cross-depth variation in potential hydrodynamic drivers during the study period: f) near-bottom current speeds, and g) wave-driven changes in pressure on the benthos. Boxplots show the median and quantile ranges, while coloured dots denote outlying values. h) Sediment reworking by parrotfishes across depth.

suggested that just 2 % of this passing sediment was deposited on the reef where it could be accumulated in turfs. The data also highlighted the marked spatial variation in sediment deposition and accumulation across the entire reef profile, with the reef flat and back reef emerging as key areas of sediment deposition and accumulation. By contrast, shallow windward reef areas at 3 and 4.5 m were found to be areas of deposition (as evidenced by sediment trap data) but with a limited capacity for sediment accumulation (as evidenced by TurfPod data). These cross-reef patterns appear to relate to wave energy and reef geomorphology, with low sediment accumulation on the windward reef crest clearly aligning with waves exerting higher energy on the benthos. Ultimately, these results are important for understanding cross-reef sediment dynamics, approaches to quantifying sediments, and the ecological implications of turf-bound sediments. These results have widespread implications for the general understanding of how coral reefs operate given that a) cross-reef profiles such as those quantified herein are a common feature of many reefs globally

(Lutzenkirchen et al., 2023), b) sediments are found on all coral reefs globally, c) changing sediment fluxes represent a key stressor (Fabricius, 2005; Wolanski et al., 2009; Andrello et al., 2022), and d) turf-bound sediments pertain to the single most abundant benthic cover on reefs today (Tebbett et al., 2023b) and likely into the future (Agostini et al., 2021; Harvey et al., 2021). Indeed, the fate of future reefs is likely to be shaped, at least in part, by turf-bound sediments (Bellwood and Fulton, 2008; Evans et al., 2020; Tebbett et al., 2021).

4.1. Cross-reef sediment dynamics

Despite only sampling over a limited temporal period, the data collected herein appears to be broadly representative of the cross-reef patterns operating in this location. For example, the cross-habitat patterns of algal turf sediment standing stock reflect those of past studies conducted up to 28 years ago at the same site (Purcell, 2000; Goatley and Bellwood, 2012), suggesting marked temporal stability in patterns of turf sediment accumulation at this location. The hydrodynamic properties quantified at Lizard Island, such as current speed and the extent of wave dissipation across the reef profile, are also reflective of data collected in past studies at the same site (Hamylton et al., 2013; Tebbett et al., 2022d). This is unsurprising given that waves and currents are heavily wind-driven at this location (Johansen, 2014) and the wind-conditions during the study were representative of the prevailing conditions at this location (Figs. S1, S2). As these lines of evidence suggest that the sediment dynamics quantified in this snapshot examination are generally characteristic of the location, they can offer important insights into how this cross-reef profile may be operating.

The cross-reef sediment dynamics quantified herein showed limited sediment deposition and accumulation on the windward slope, higher deposition (relative to the slope) but very low accumulation on the shallow crest/outer-flat (3–4.5 m), and high sediment accumulation and/or deposition on the mid-flat and back reef. Given the prevailing winds and hydrodynamics, such cross-reef patterns are largely indicative of sediment movement away from the high-energy windward reef crest environment, towards the lower-energy flat and sheltered back reef habitat. Importantly, this inference about the direction of sediment movement also aligns with previous studies that have documented similar patterns across coral reefs and have suggested that the interaction between waves and reef geomorphology is key in defining the sedimentary context for reef habitats (e.g. Kench and Brander, 2006; Browne et al., 2013b; Pomeroy et al., 2018, 2021). Our results support these inferences and extend the findings to sediment deposition and accumulation in turfs on reefs, with the interaction between waves and geomorphology being key in the maintenance of a reef crest habitat with low turf sediment loads. As this habitat has the highest benthic productivity, per unit area (Klumpp and McKinnon, 1989; Russ, 2003), and supports the highest herbivore densities and herbivory rates (Lewis and Wainwright, 1985; Bellwood et al., 2018), the maintenance of low sediments in this zone has a variety of important ecological implications (discussed below). Further insights into the interactions between sediments, geomorphology, and hydrodynamics may also be gleaned by considering how the data align with that of a previous study which used similar methods but applied them under a fundamentally different context.

4.2. Offshore versus inshore cross-study comparison

A recent study used similar methods to those used herein to quantify sediment dynamics at Orpheus Island, an inshore reef on the GBR (Schlaefer et al., 2022). However, it is critical to note that our study location at Lizard Island differs markedly from the location studied at Orpheus Island in Schlaefer et al. (2022) in terms of: i) wave exposure (windward versus leeward); ii) shelf-position and proximity to the mainland (mid-shelf Lizard ~30 km from the mainland versus inner-shelf Orpheus ~15 km from the mainland); and iii) reef geomorphology, whereby Lizard Island is composed of a reef slope (rising from ~30 m depth including a full cross-reef profile into a lagoon), while Orpheus Island is an island attached fringing reef (with a slope rising from ~15 m depth) (Fig. 4). Given the similarity of the methods used, but the markedly different contexts under which they were applied, consideration of our results relative to those of Schlaefer et al. (2022) is warranted. A detailed comparison can be found in the supplemental material (Text S3), however, below we consider how our results align with the two principal findings of Schlaefer et al. (2022): a) the relative quantities and strength of fluxes between different sediment reservoirs, and b) the existence of a highly-dynamic, high sediment deposition and accumulation regime at 3 m driven by wave energy.

At the clear-water, windward Lizard Island location studied here, the standing stock of sediment in the water column and in turfs, was far lower than at the more turbid, leeward Orpheus Island location (stocks were 80 % and 310 % higher at Orpheus Island, respectively [Fig. 4]). Importantly, these differences in standing stocks align with past studies of turbidity gradients across the GBR (Fabricius et al., 2014), as well as standing stock sediment loads in turfs, and on the benthos, across the GBR (Fabricius and De'ath, 2001; Tebbett et al., 2017a). In terms of fluxes, sediment accumulation in traps was also 290 % higher at Orpheus Island (Fig. 4), potentially suggesting stronger links between the water column sediment reservoir and the on-reef sediment reservoir at Orpheus compared to Lizard. However, despite the marked differences in standing stocks and trapping rates, the total sediment load travelling over the reef in the water column was remarkably similar at both Lizard and Orpheus, with it being just 10 % higher at Orpheus Island (Fig. 4).

Given the different environmental contexts in which Lizard Island and Orpheus Island exist, especially in terms of suspended sediment concentrations being 80 % higher at Orpheus Island, it is interesting how similar the estimates of total sediment load/delivery in the water column are (Fig. 4). Consideration of these two properties (i.e. total load versus concentration) of water column sediments is important because most past coral reef studies focus on measures of sediment concentration, rather than estimates of total delivery (reviewed in Schlaefer et al., 2021). As such, it can be unclear which mechanism (i.e. suspended sediment concentration versus total sediment delivery) aligns more closely with on-reef sediment dynamics. This comparison between studies using similar methods suggests that the former (i.e. suspended sediment concentration) may correlate more directly to on-reef sediment processes, since both suspended sediment concentration and deposition in traps were higher at Orpheus Island. While this inference is based on just two locations, the notion that increased suspended sediment concentrations translate directly to increased benthic sediment loads is supported by previous evidence. For example, past studies have found that increased suspended sediment concentrations via flood plumes (Storlazzi et al., 2009; Golbuu et al., 2011), dredging activity (Miller et al., 2016; Jones et al., 2019), and local hydrodynamic activity (Castro et al., 2012; Whinney et al., 2017) all translate to increased sediment deposition on coral reefs. However, it is important to note that this deposition is invariably embedded in a spatial context and we must also consider the cross-depth patterns.

At the leeward study site on Orpheus Island, Schlaefer et al. (2022) documented a highly dynamic high sediment movement regime at 3 m and a less dynamic, lower sediment movement regime at 4.5–12 m, with the delineation of these two regimes supporting the occurrence of a shallow 'resuspension zone' and a deeper 'sedimentation zone' described in Wolanski et al. (2005). Importantly, in Schlaefer et al. (2022) both sediment trapping rates, and TurfPod accumulation rates peaked at 3 m, which was suggestive of both high sediment deposition and accumulation in turfs. This pattern was not supported by cross-depth data from the windward Lizard Island location quantified herein, as only sediment trapping rates peaked at 3 m and declined with depth, while TurfPod accumulation was lowest at 3 m and increased until 6 m before leveling out. Unlike Orpheus, the data from Lizard, therefore, suggests that there is limited capacity for sediment accumulation in turfs at 3–4.5 m, which may be the result of the interaction between waves and reef geomorphology.

The interaction between wave energy and reef geomorphology is a well-known driver of sediment dynamics (Larcombe et al., 2001; Storlazzi et al., 2009; Golbuu et al., 2011) and it is this interaction that probably shaped the

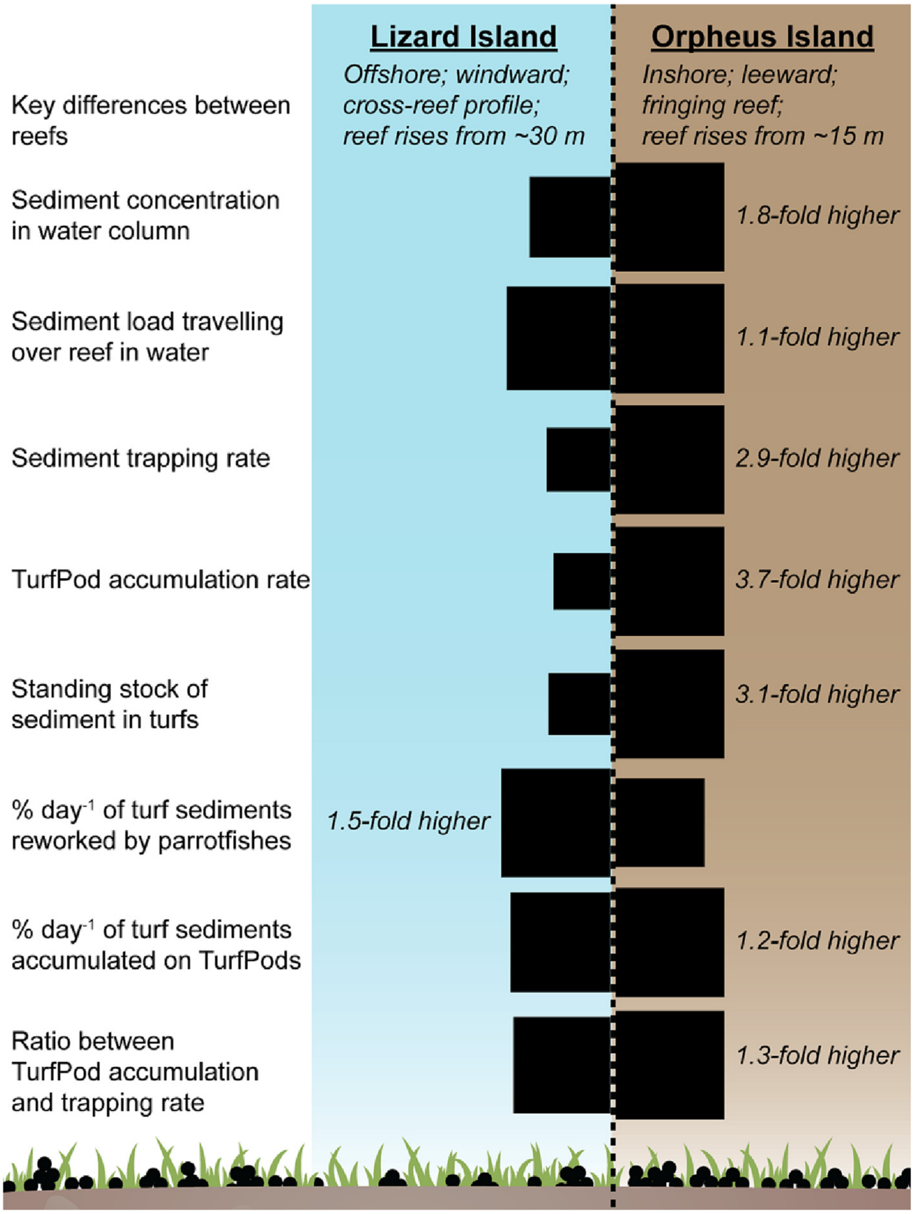

Fig. 4. Conceptual schematic showing the relative amount of sediment in different reservoirs and the relative strength of sedimentary fluxes quantified at the scale of the 'total reef section' in the present study, as well as in a past study by Schlaefer et al. (2022) that used similar methods. Note the lower sediment trapping and accumulation rates at Lizard Island. The area of the black boxes denotes the relative differences in magnitudes between the two locations.

differential patterns of sediment accumulation on TurfPods documented here versus at Orpheus Island in Schlaefer et al. (2022). This is because, at Orpheus Island, wave energy is far lower than at Lizard Island (Fig. S5d). Furthermore, the Orpheus Island study site was a fringing reef with a relatively narrow flat (~50 m) and a slope that only reached a depth of approximately 15 m. This means that, at Orpheus Island, there is less potential for wave-driven sediment resuspension and advection (also see Wolanski et al., 2005 for a comparison on resuspension at leeward versus windward reefs). If sediments are resuspended at Orpheus Island, it is harder for them to move out of the system, since the reef fringes an island and thus lacks an expansive reef flat and back reef, potentially leading to higher recycling in the shallow narrow reef flat (cf. Ogston et al., 2004; Lambrechts et al., 2010). By contrast, at Lizard Island, wave energy was ~3-fold higher than at Orpheus Island, the reef flat was approximately 400 m wide and backed onto a lagoonal back reef, and the reef slope reached a depth of >30 m. This means that there is more potential for sediment to be resuspended and entrained across the flat (as discussed above) or transported into depths where it is exported from the system once it is below the depth of the resuspension zone (cf. Wolanski et al., 2005, 2008; Morgan and Kench, 2014). Ultimately, these differences between locations suggests that the 'post-settlement' fate of sediments, especially in terms of their accumulation in turfs, is dependent on local conditions, especially wave energy and geomorphology. Local hydrodynamic and geomorphological constraints may, therefore, predispose some reefs or reef areas to high-load stagnant sediment regimes, while others remain relatively sediment free, even at equivalent depths.

The marked context-dependent nature of sediment accumulation on reefs, even over a few meters at the spatial scale of a single reef profile, and the clear interaction between multiple drivers such as hydrodynamics and geomorphology, means that modelling these dynamics is a difficult task. This problem is further compounded when the potential for temporal variability in sediment dynamics, and the underlying drivers, is considered (e.g. Brander et al., 2004; Victor et al., 2006; Storlazzi et al., 2009; Browne et al., 2013a). Nevertheless, progress has been made in modelling suspended sediment dynamics over large spatial scales (reviewed in Horner-Devine et al., 2015), with large-scale remote sensing data being useful for informing these models (e.g. Margvelashvili et al., 2013). Moreover, advances in sediment transport modelling have facilitated insights into sediment plume dispersal and how these plumes interact with coral reefs (e.g. Suárez-Castro et al., 2021; Andrello et al., 2022). However, we are only just starting to unravel the links between suspended sediment concentrations, sedimentation, and accumulation on reefs, especially in turfs. The present study, as well as past research (e.g. Latrille et al., 2019; Schlaefer et al., 2022), suggests these links are complex. This complexity is further magnified by the fact that unlike suspended sediment concentrations, for which largescale data is readily available, the quantification of on-reef sediment accumulation is far more challenging and labour intensive (Tebbett et al., 2022b). The methods commonly used to quantify sediment deposition/accumulation, such as sediment traps, may also provide biased insights into this process on reefs (discussed below). Despite these challenges, developing a predictive model for sediment accumulation on reefs will be important given its ecological consequences (discussed below). This endeavour will invariably require the development of less labour intensive methods to collect data across large spatial scales to help ground-truth models.

4.3. Methodological implications

Sediment traps are the most widely used tool for quantifying sedimentary processes on reefs (Schlaefer et al., 2021). However, this widespread use has been criticised because it has been suggested that data from sediment traps only provides a partial insight into sedimentary processes, and that such data are not necessarily informative for on-reef benthic processes (Storlazzi et al., 2011). This is because the relative elevation of the sediment traps above the substratum, means that they have relatively weak links with benthic sediments and instead generally capture sediment from the water column (see Bothner et al., 2006; Storlazzi et al., 2011; Latrille et al., 2019; Ng et al., 2022). Moreover, the design of sediment traps means that they prohibit the resuspension of sediments trapped inside them (Storlazzi et al., 2011). Therefore, it has been suggested that sediment traps specifically factor out the capacity for waves and other hydrodynamic drivers to resuspend and redistribute sediments and, cannot be used for understanding on-reef sediment processes (Storlazzi et al., 2011; Latrille et al., 2019). The data in the present study support these suggestions.

The divergent trajectories documented for sediment trapping rates and sediment accumulation on TurfPods across the depth gradient examined suggest that sediment traps can yield biased insights into on-reef sediment accumulation. If inferences herein were only based on sediment trap data, then it would have been concluded that the 3 and 4.5 m depths at Lizard Island were areas of high sediment deposition and accumulation. Clearly this was not the case. When the data from TurfPods were considered, it was evident that little sediment accumulation occurs at 3 and 4.5 m at Lizard Island. Importantly, TurfPods allow both the deposition and resuspension of sediments, as in SedPods (Field et al., 2013). However, the artificial turf attached to the TurfPods is designed to mimic the capacity of naturally occurring turfs to retain sediments during resuspension events (Latrille et al., 2019) (see Text S4 for further discussion). Importantly, the six-day deployment period used here means that the TurfPods were highly unlikely to have reached a saturation point (see Latrille et al., 2019), which means that these data represent a time-averaged continuous accumulation rate for the study period. In addition, the lower profile of TurfPods at just 7 cm high, means that they have far stronger links to the benthos than the 60 cm high sediment traps (Latrille et al., 2019; Ng et al., 2022). As a result, these data highlight the value in using multiple methods to examine sediment dynamics on reefs, and caution against the use of sediment traps exclusively when the purpose of a study is to understand sediment accumulation and benthic processes.

It is also important to note that the type of sedimentary metrics quantified can yield differing insights into sediment dynamics on reefs. In the present study, we focused on total sediment loads because, in terms of turf-based sediments and their ecological implications, it generally has the largest effect, while sediment type and grain size are of secondary importance (Bellwood and Fulton, 2008; Gordon et al., 2016; Tebbett et al., 2017b, 2020). Moreover, due to the relatively short deployment period used in the present study (which was essential to ensure a tight temporal coupling between the quantification of sediment trapping/accumulation rates and the bio-physical drivers examined) the absolute amounts of sediment collected were relatively small, prohibiting detailed granulometric analyses such as via a laser particle analyser. Nevertheless, previous research has suggested that the size of sediments accumulated in traps differs from that on the benthos (Bothner et al., 2006; Storlazzi et al., 2011; Latrille et al., 2019; Ng et al., 2022). By contrast, the grain size distribution of sediments that accumulate on TurfPods have been found to align more closely with the sediments in natural turfs (Latrille et al., 2019). Nevertheless, to provide further insights into sediment dynamics on reefs, combining the quantification of sediments over a longer temporal period (to allow greater sediment trapping rates) with more in-depth examination of sediment properties such as grain size would be useful. Although, such quantification would invariably mean the coupling between the bio-physical drivers quantified, and the sedimentary processes examined, may be weaker.

4.4. Ecological implications

Given that a link may exist between suspended sediment concentrations and sediment accumulation on the benthos, further investigation of this link is particularly important for advancing the understanding of reef ecology. This is because ecological studies often examine correlations between turbidity and variables such as fish abundance/composition (Mallela et al., 2007; Bejarano and Appeldoorn, 2013; Cheal et al., 2013; Moustaka et al., 2018), benthic organisms (Fabricius et al., 2005; Moustaka et al., 2019; Santana et al., 2023), or coral settlement (Evans et al., 2020; Thomson et al., 2021). However, when correlations between turbidity and ecological variables are found, at least some are likely to be partially driven by the amount of sediment accumulated on the benthos, rather than in the water column, per se. Arguably, herbivorous fishes provide the best example of this phenomenon since their abundance and/or community composition is often negatively correlated with turbidity (Mallela et al., 2007; Bejarano and Appeldoorn, 2013; Cheal et al., 2013; Moustaka et al., 2018). However, these fishes spend most of the day grazing on the reef substratum, where they directly interact with sediments (Bellwood and Fulton, 2008; Adam et al., 2018; Duran et al., 2019; Pessarrodona et al., 2022). Interestingly, there is now a broad consensus that sediments accumulated in turfs can constrain feeding by (Goatley and Bellwood, 2012; Tebbett et al., 2020; Ng et al., 2021; Akita et al., 2022) and nutritional resource yields to (Gordon et al., 2016; Tebbett et al., 2018) herbivorous fishes, with potential bottom-up effects on their assemblages (Tebbett et al., 2021). The fish data from the present study supports this notion as species known to be particularly sensitive to the effects of algal turf sediments, such as the surgeonfish *Ctenochaetus striatus* (Tebbett et al., 2020), typified the low-sediment Lizard Island location (Fig. S6).

Interestingly, wave energy and reef geomorphology have also been highlighted as key factors related to herbivorous fish distributions previously (Bejarano et al., 2017; Bennett et al., 2018; Roff et al., 2019; Samoilys et al., 2019). Given that these factors also appear to be key in shaping sediment distributions on reefs, it may be important to tease apart how these factors are intertwined, especially in a more comprehensive spatial context. This would be particularly useful in further elucidating the hydrodynamic and geomorphic context for reefs, helping to identify their susceptibility to sediment disturbances. This facet could also be explored from an evolutionary perspective, as it has been suggested that a major breakthrough in the evolutionary history of herbivorous fishes was their capacity to move into shallow, high-energy, coral reef habitats (Bellwood et al., 2014, 2017). This would have been evolutionarily advantageous from a nutritional perspective given the limited capacity for such areas to accumulate sediments, and could help explain why large-bodied herbivorous reef fishes have outpaced all other trophic groups in recent diversification rates (Siqueira et al., 2020).

The ecological interactions between sediments and herbivorous fishes on coral reefs also brings to the fore the potential importance of fish-derived geo-ecological functions, especially sediment reworking (Stoddart, 1969; Bellwood et al., 2003; Perry et al., 2022). The role of parrotfishes is now widely appreciated in these functions, with the same methods as those used herein being applied to explore their ecology in a variety of different contexts (Hoey and Bellwood, 2008; Morgan and Kench, 2016; Yarlett et al., 2018; Morais et al., 2022). However, despite the importance of other reef fish groups in sediment transport being recognised over 60 years ago (Bardach, 1961), developing methods to readily estimate their roles has lagged behind parrotfishes (Perry et al., 2022). Further quantification of the role of surgeonfishes in geo-ecological functions may thus be a particularly fertile avenue for future research. Currently, the role of just a single species, *Ctenochaetus striatus*, has been rigorously quantified (Goatley and Bellwood, 2010; Krone et al., 2011), although at least 30 surgeonfish species are likely to play a major role in the transport of sediment around reefs (reviewed in Tebbett et al., 2022c). As these sediment transporting species can be particularly abundant in some contexts (Fig. S6), further insights into the magnitude of their effects would be important in developing a comprehensive understanding of the biological drivers of sediment dynamics on coral reefs.

Ultimately, the ecological implications of our findings are widespread and multifaceted. This is because on-reef sediments in turfs represent the indirect medium through which hydrodynamics and reef geomorphology shape the ecological functioning of reefs. Indeed, from tropical coral reefs to temperate reef systems, sediments in turfs have been found to modulate/relate to: herbivory/detritivory rates (Goatley and Bellwood, 2012; Ng et al., 2021; Akita et al., 2022), growth and production of primary producers (Irving and Connell, 2002; Clausing et al., 2014; Tebbett and Bellwood, 2020), settlement of critical habitat-forming organisms (Birrell et al., 2005; Watanabe et al., 2016; Layton et al., 2019; Speare et al., 2019), competitive benthic interactions (Steneck, 1997; O'Brien and Scheibling, 2018; Liao et al., 2019), cryptofauna abundance (Prathep et al., 2003; Logan et al., 2008; Kramer et al., 2012), and detrital quality (Purcell and Bellwood, 2001; Tebbett et al., 2021). All of these factors are, or are linked to, critical ecosystem processes that lie at the foundations of how reefs operate (Bellwood et al., 2019; Brandl et al., 2019) or recover from disturbances (Holbrook et al., 2018; Evans et al., 2020). Yet, because turf sediments are largely unquantified in ecological studies and unmonitored, we are only just beginning to appreciate the relative strength and context dependency of interactions between turf sediments and the functioning of reef systems. This is despite turfs being the single most abundant benthic covering on most shallow reef systems globally (Filbee-Dexter and Wernberg, 2018; Tebbett et al., 2023b), with their abundance likely to increase under future reef conditions (Agostini et al., 2021; Harvey et al., 2021).

5. Conclusions

By simultaneously quantifying a range of sediment reservoirs and modifying processes across a windward reef profile, our study revealed several key insights. Firstly, despite enough sediment passing over the reef to replace all turf-bound sediment in just 8 h, only an estimated 2 % of this passing sediment was deposited onto the reef. Moreover, patterns of sediment deposition and subsequent accumulation were embedded in a distinct spatial arrangement. This inference, however, was only revealed based on data from TurfPods, given that sediment traps factored out resuspension of sediments and did not reflect on-reef sediment accumulation. When considered in light of past research conducted on a leeward turbid reef, the data suggests that increased sediment concentrations, rather than total suspended sediment load, translate more directly into higher sediment deposition rates. From an ecological perspective, these results suggest that the context of the reef in question will ultimately determine the extent to which sediment deposition will translate into on-reef sediment accumulation in algal turfs. Indeed, wave energy and reef geomorphology appear to be key in the maintenance of the low turf sediment, ecologically critical, reef crest habitat. Given that algal turfs act as a key ecological interface on most reefs globally (Connell et al., 2014), and their coverage is poised to increase (Agostini et al., 2021; Tebbett et al., 2023a), these results have far reaching implications for our understanding of how reefs will function in the near future.

CRediT authorship contribution statement

Sterling B. Tebbett: Conceptualization, Data curation, Formal analysis, Investigation, Methodology, Visualization, Writing – original draft. **Jodie A. Schlaefer:** Conceptualization, Data curation, Formal analysis, Investigation, Methodology, Visualization, Writing – review & editing. **Casey L. Bowden:** Conceptualization, Investigation, Writing – review & editing. **William P. Collins:** Conceptualization, Investigation, Writing – review & editing. **Christopher R. Hemingson:** Conceptualization, Investigation, Writing – review & editing. **Scott D. Ling:** Conceptualization, Writing – review & editing. **Juliano Morais:** Conceptualization, Investigation, Writing – review & editing. **Renato A. Morais:** Conceptualization, Investigation, Methodology, Writing – review & editing. **Alexandre C. Siqueira:** Conceptualization, Investigation, Writing – review & editing. **Robert P. Streit:** Conceptualization, Investigation, Methodology, Writing – review & editing. **Sam Swan:** Conceptualization, Data curation, Investigation, Visualization, Writing – review & editing. **David R. Bellwood:** Conceptualization, Funding acquisition, Methodology, Resources, Supervision, Writing – review & editing.

Data availability

Data will be made available on request.

Declaration of competing interest

The authors declare that they have no known competing financial interests or personal relationships that could have appeared to influence the work reported in this paper.

Acknowledgements

We thank Shaun Robinson (Concrete Laboratory, James Cook University), and Rachael and Simon Macdonald (Marine Geophysics Laboratory, James Cook University), for logistical support; Lizard Island Research Station staff and Phil Osmond for field support; Georgia Robinson for assistance processing samples; two anonymous reviewers for constructive feedback; and Joanna Woerner and Tracey Saxby, Integration and Application Network for vector images.

Funding

This work was supported by the Australian Research Council (DRB, CE140100020 and FL190100062; SDL, FT200100949), the Ian Potter Foundation (SBT), and the Australian Museum's Lizard Island Research Station (SBT).

Appendix A. Supplementary data

Supplementary data to this article can be found online at https://doi.org/10.1016/j.scitotenv.2023.165188.

References

Adam, T.C., Duran, A., Fuchs, C.E., Roycroft, M.V., Rojas, M.C., Ruttenberg, B.I., Burkepile, D.E., 2018. Comparative analysis of foraging behavior and bite mechanics reveals complex functional diversity among Caribbean parrotfishes. Mar. Ecol. Prog. Ser. 597, 207–220.

Agostini, S., Harvey, B.P., Milazzo, M., Wada, S., Kon, K., Floc'h, N., Komatsu, K., Kuroyama, M., Hall-Spencer, J.M., 2021. Simplification, not "tropicalization", of temperate marine ecosystems under ocean warming and acidification. Glob. Chang. Biol. 27, 4771–4784.

Akita, Y., Kurihara, T., Uehara, M., Shiwa, T., Iwai, K., 2022. Impacts of overfishing and sedimentation on the feeding behavior and ecological function of herbivorous fishes in coral reefs. Mar. Ecol. Prog. Ser. 686, 141–157.

Albert, S., Udy, J., Tibbetts, I.R., 2008. Responses of algal communities to gradients in herbivore biomass and water quality in Marovo Lagoon, Solomon Islands. Coral Reefs 27, 73–82.

Andrello, M., Darling, E.S., Wenger, A., Suárez-Castro, A.F., Gelfand, S., Ahmadia, G.N., 2022. A global map of human pressures on tropical coral reefs. Conserv. Lett. 15, e12858.

Bainbridge, Z., Lewis, S., Bartley, R., Fabricius, K., Collier, C., Waterhouse, J., Garzon-Garcia, A., Robson, B., Burton, J., Wenger, A., Brodie, J., 2018. Fine sediment and particulate organic matter: a review and case study on ridge-to-reef transport, transformations, fates, and impacts on marine ecosystems. Mar. Pollut. Bull. 135, 1205–1220.

Bardach, J.E., 1961. Transport of calcareous fragments by reef fishes. Science 133, 98–99.

Bejarano, I., Appeldoorn, R., 2013. Seawater turbidity and fish communities on coral reefs of Puerto Rico. Mar. Ecol. Prog. Ser. 474, 217–226.

Bejarano, S., Jouffray, J.-B., Chollett, I., Allen, R., Roff, G., Marshell, A., Steneck, R., Ferse, S., Mumby, P.J., 2017. The shape of success in a turbulent world: wave exposure filtering of coral reef herbivory. Funct. Ecol. 6, 1312–1324.

Bellwood, D.R., 1996. Production and reworking of sediment by parrotfishes (family Scaridae) on the Great Barrier Reef, Australia. Mar. Biol. 125, 795–800.

Bellwood, D.R., Choat, J.H., 1990. A functional analysis of grazing in parrotfishes (family Scaridae): the ecological implications. Environ. Biol. Fish 28, 189–214.

Bellwood, D.R., Fulton, C.J., 2008. Sediment-mediated suppression of herbivory on coral reefs: decreasing resilience to rising sea levels and climate change? Limnol. Oceanogr. 53, 2695–2701.

Bellwood, D.R., Hoey, A.S., Choat, J.H., 2003. Limited functional redundancy in high diversity systems: resilience and ecosystem function of coral reefs. Ecol. Lett. 6, 281–285.

Bellwood, D.R., Goatley, C.H.R., Brandl, S.J., Bellwood, O., 2014. Fifty million years of herbivory on coral reefs: fossils, fish and functional innovations. Proc R. Soc. B Biol. Sci. 281, 20133046.

Bellwood, D.R., Goatley, C.H.R., Bellwood, O., 2017. The evolution of fishes and corals on reefs: form, function and interdependence. Biol. Rev. 92, 878–901.

Bellwood, D.R., Tebbett, S.B., Bellwood, O., Mihalitsis, M., Morais, R.A., Streit, R.P., Fulton, C.J., 2018. The role of the reef flat in coral reef trophodynamics: past, present, and future. Ecol. Evol. 8, 4108–4119.

Bellwood, D.R., Streit, R.P., Brandl, S.J., Tebbett, S.B., 2019. The meaning of the term 'function' in ecology: a coral reef perspective. Funct. Ecol. 33, 948–961.

Bennett, S., Halford, A.R., Choat, J.H., Hobbs, J.-P.A., Santana-Garcon, J., Ayling, A.M., Harvey, E.S., Newman, S.J., 2018. Geography and island geomorphology shape fish assemblage structure on isolated coral reef systems. Ecol. Evol. 8, 6242–6252.

Birrell, C.L., McCook, L.J., Willis, B.L., 2005. Effects of algal turfs and sediment on coral settlement. Mar. Pollut. Bull. 51, 408–414.

Bonaldo, R.M., Bellwood, D.R., 2008. Size-dependent variation in the functional role of the parrotfish *Scarus rivulatus* on the Great Barrier Reef, Australia. Mar. Ecol. Prog. Ser. 360, 237–244.

Bothner, M.H., Reynolds, R.L., Casso, M.A., Storlazzi, C.D., Field, M.E., 2006. Quantity, composition, and source of sediment collected in sediment traps along the fringing coral reef off Molokai, Hawaii. Mar. Pollut. Bull. 52, 1034–1047.

Bowden, C.L., Streit, R.P., Bellwood, D.R., Tebbett, S.B., 2022. A 3D perspective on sediment turnover and feeding selectivity in blennies. Mar. Pollut. Bull. 180, 113799.

Brander, R.W., Kench, P.S., Hart, D., 2004. Spatial and temporal variations in wave characteristics across a reef platform, Warraber Island, Torres Strait, Australia. Mar. Geol. 207, 169–184.

Brandl, S.J., Rasher, D.B., Côté, I.M., Casey, J.M., Darling, E.S., Lefcheck, J.S., Duffy, J.E., 2019. Coral reef ecosystem functioning: eight core processes and the role of biodiversity. Front. Ecol. Environ. 17, 445–454.

Brooks, M.E., Kristensen, K., van Benthem, K.J., Magnusson, A., Berg, C.W., Nielsen, A., Skaug, H.J., Machler, M., Bolker, B.M., 2017. glmmTMB balances speed and flexibility among packages for zero-inflated generalized linear mixed modeling. R J. 9, 378–400.

Browne, N.K., Smithers, S.G., Perry, C.T., 2013a. Spatial and temporal variations in turbidity on two inshore turbid reefs on the Great Barrier Reef, Australia. Coral Reefs 32, 195–210.

Browne, N.K., Smithers, S.G., Perry, C.T., 2013b. Carbonate and terrigenous sediment budgets for two inshore turbid reefs on the central Great Barrier Reef. Mar. Geol. 346, 101–123.

Cartwright, P.J., Fearns, P.R.C.S., Branson, P., Cuttler, M.V.W., O'Leary, M., Browne, N.K., Lowe, R.J., 2021. Identifying metocean drivers of turbidity using 18 years of MODIS satellite data: implications for marine ecosystems under climate change. Remote Sens. 13, 3616.

Cartwright, P.J., Iles, J.A., Mattone, C., O'Callaghan, M., Waltham, N.J., 2022. Turbidity (NTU) to Suspended Sediment Concentration (SSC) Conversion Protocol: Technical Report. James Cook University Press, Townsville, Australia.

Castro, C.B., Segal, B., Negrão, F., Calderon, E.N., 2012. Four-year monthly sediment deposition on turbid southwestern Atlantic coral reefs, with a comparison of benthic assemblages. Braz. J. Oceanogr. 60, 49–63.

Cheal, A.J., Emslie, M., MacNeil, M.A., Miller, I., Sweatman, H., 2013. Spatial variation in the functional characteristics of herbivorous fish communities and the resilience of coral reefs. Ecol. Appl. 23, 174–188.

Clausing, R.J., Annunziata, C., Baker, G., Lee, C., Bittick, S.J., Fong, P., 2014. Effects of sediment depth on algal turf height are mediated by interactions with fish herbivory on a fringing reef. Mar. Ecol. Prog. Ser. 517, 121–129.

Cleary, D.F.R., Polónia, A.R.M., Renema, W., Hoeksema, B.W., Rachello-Dolmen, P.G., Moolenbeek, R.G., Budiyanto, A., Yahmantoro, Tuti, Y., Giyanto, Draisma, S.G.A., Prud'homme van Reine, W.F., Hariyanto, R., Gittenberger, A., Rikoh, M.S., de Voogd, N.J., 2016. Variation in the composition of corals, fishes, sponges, echinoderms, ascidians, molluscs, foraminifera and macroalgae across a pronounced in-to-offshore environmental gradient in the Jakarta Bay–Thousand Islands coral reef complex. Mar. Pollut. Bull. 110, 701–717.

Connell, S.D., Foster, M.S., Airoldi, L., 2014. What are algal turfs? Towards a better description of turfs. Mar. Ecol. Prog. Ser. 495, 299–307.

Davidson, J., Thompson, A., Logan, M., Schaffelke, B., 2019. High spatio-temporal variability in Acroporidae settlement to inshore reefs of the great barrier reef. PLoS ONE 14, e0209771.

Devlin, M., Schaffelke, B., 2009. Spatial extent of riverine flood plumes and exposure of marine ecosystems in the Tully coastal region, Great Barrier Reef. Mar. Freshw. Res. 60, 1109.

Doropoulos, C., Gómez-Lemos, L.A., Salee, K., McLaughlin, M.J., Tebben, J., Van Koningsveld, M., Feng, M., Babcock, R.C., 2022. Limitations to coral recovery along an environmental stress gradient. Ecol. Appl. 32, e2558.

Duran, A., Adam, T.C., Palma, L., Moreno, S., Collado-Vides, L., Burkepile, D.E., 2019. Feeding behavior in Caribbean surgeonfishes varies across fish size, algal abundance, and habitat characteristics. Mar. Ecol. 40, e12561.

Evans, R.D., Wilson, S.K., Fisher, R., Ryan, N.M., Babcock, R., Blakeway, D., Bond, T., Dorji, P., Dufois, F., Fearns, P., Lowe, R.J., Stoddart, J., Thomson, D.P., 2020. Early recovery dynamics of turbid coral reefs after recurring bleaching events. J. Environ. Manag. 268, 110666.

Fabricius, K.E., 2005. Effects of terrestrial runoff on the ecology of corals and coral reefs: review and synthesis. Mar. Pollut. Bull. 50, 125–146.

Fabricius, K., De'ath, G., 2001. Environmental factors associated with the spatial distribution of crustose coralline algae on the Great Barrier Reef. Coral Reefs 19, 303–309.

Fabricius, K.E., De'ath, G., McCook, L., Turak, E., Williams, D.M., 2005. Changes in algal, coral and fish assemblages along water quality gradients on the inshore Great Barrier Reef. Mar. Pollut. Bull. 51, 384–398.

Fabricius, K.E., Logan, M., Weeks, S., Brodie, J.E., 2014. The effects of river run-off on water clarity across the central Great Barrier Reef. Mar. Pollut. Bull. 84, 191–200.

Fabricius, K.E., Logan, M., Weeks, S.J., Lewis, S.E., Brodie, J., 2016. Changes in water clarity in response to river discharges on the Great Barrier Reef continental shelf: 2002-2013. Estuar. Coast. Shelf Sci. 173, A1–A15.

Field, M.E., Chezar, H., Storlazzi, C.D., 2013. SedPods: a low-cost coral proxy for measuring net sedimentation. Coral Reefs 32, 155–159.

Filbee-Dexter, K., Wernberg, T., 2018. Rise of turfs: a new battlefront for globally declining kelp forests. BioScience 68, 64–76.

Goatley, C.H.R., Bellwood, D.R., 2010. Biologically mediated sediment fluxes on coral reefs: sediment removal and off-reef transportation by the surgeonfish *Ctenochaetus striatus*. Mar. Ecol. Prog. Ser. 415, 237–245.

Goatley, C.H.R., Bellwood, D.R., 2012. Sediment suppresses herbivory across a coral reef depth gradient. Biol. Lett. 8, 1016–1018.

Golbuu, Y., Victor, S., Wolanski, E., Richmond, R.H., 2003. Trapping of fine sediment in a semi-enclosed bay, Palau, Micronesia. Estuar. Coast. Shelf Sci. 57, 941–949.

Golbuu, Y., Wolanski, E., Harrison, P., Richmond, R.H., Victor, S., Fabricius, K.E., 2011. Effects of land-use change on characteristics and dynamics of watershed discharges in Babeldaob, Palau, Micronesia. J. Mar. Biol. 2011, 981273.

Gordon, S.E., Goatley, C.H.R., Bellwood, D.R., 2016. Low-quality sediments deter grazing by the parrotfish *Scarus rivulatus* on inner-shelf reefs. Coral Reefs 35, 285–291.

Grant, W.D., Madsen, O.S., 1979. Combined wave and current interaction with a rough bottom. J. Geophys. Res. Oceans 84, 1797–1808.

Hamylton, S.M., Pescud, A., Leon, J.X., Callaghan, D.P., 2013. A geospatial assessment of the relationship between reef flat community calcium carbonate production and wave energy. Coral Reefs 32, 1025–1039.

Harborne, A.R., Rogers, A., Bozec, Y.-M., Mumby, P.J., 2017. Multiple stressors and the functioning of coral reefs. Annu. Rev. Mar. Sci. 9, 445–468.

Harris, D.L., Vila-Concejo, A., Webster, J.M., 2014. Geomorphology and sediment transport on a submerged back-reef sand apron: One Tree Reef, Great Barrier Reef. Geomorphology 222, 132–142.

Hartig, F., 2020. DHARMa: Residual Diagnostics for Hierarchical (Multi-Level/Mixed) Regression Models R package version 0.3.3.0.

Harvey, B.P., Allen, R., Agostini, S., Hoffmann, L.J., Kon, K., Summerfield, T.C., Wada, S., Hall-Spencer, J.M., 2021. Feedback mechanisms stabilise degraded turf algal systems at a CO_2 seep site. Commun. Biol. 4, 219.

Hijmans, R.J., 2022. geosphere: Spherical Trigonometry R package version 1.5-18.

Hoey, A.S., 2018. Feeding in parrotfishes: the influence of species, body size, and temperature. In: Hoey, A.S., Bonaldo, R.M. (Eds.), Biology of Parrotfishes. Taylor & Francis, Boca Raton, pp. 119–133.

Hoey, A.S., Bellwood, D.R., 2008. Cross-shelf variation in the role of parrotfishes on the Great Barrier Reef. Coral Reefs 27, 37–47.

Holbrook, S.J., Adam, T.C., Edmunds, P.J., Schmitt, R.J., Carpenter, R.C., Brooks, A.J., Lenihan, H.S., Briggs, C.J., 2018. Recruitment drives spatial variation in recovery rates of resilient coral reefs. Sci. Rep. 8, 7338.

Horner-Devine, A.R., Hetland, R.D., MacDonald, D.G., 2015. Mixing and transport in coastal river plumes. Annu. Rev. Fluid Mech. 47, 569–594.

Hughes, T.P., Barnes, M.L., Bellwood, D.R., Cinner, J.E., Cumming, G.S., Jackson, J.B.C., Kleypas, J., Leemput, I.A. van de, Lough, J.M., Morrison, T.H., Palumbi, S.R., Nes, E.H.V., Scheffer, M., 2017. Coral reefs in the Anthropocene. Nature 546, 82–90.

Irving, A.D., Connell, S.D., 2002. Interactive effects of sedimentation and microtopography on the abundance of subtidal turf-forming algae. Phycologia 41, 517–522.

Jing, L., Ridd, P.V., 1996. Wave-current bottom shear stresses and sediment resuspension in Cleveland Bay, Australia. Coast. Eng. 29, 169–186.

Johansen, J.L., 2014. Quantifying water flow within aquatic ecosystems using load cell sensors: a profile of currents experienced by coral reef organisms around Lizard Island, Great Barrier Reef, Australia. PLoS ONE 9, e83240.

Jones, R., Fisher, R., Stark, C., Ridd, P., 2015. Temporal patterns in seawater quality from dredging in tropical environments. PLoS ONE 10, e0137112.

Jones, R., Fisher, R., Bessell-Browne, P., 2019. Sediment deposition and coral smothering. PLoS ONE 14, e0216248.

Jouffray, J.B., Wedding, L.M., Norström, A.V., Donovan, M.K., Williams, G.J., Crowder, L.B., Erickson, A.L., Friedlander, A.M., Graham, N.A.J., Gove, J.M., Kappel, C.V., Kittinger, J.N., Lecky, J., Oleson, K.L.L., Selkoe, K.A., White, C., Williams, I.D., Nyström, M., 2019. Parsing human and biophysical drivers of coral reef regimes. Proc. R. Soc. B Biol. Sci. 286, 20182544.

Kench, P.S., Brander, R.W., 2006. Wave processes on coral reef flats: implications for reef geomorphology using Australian case studies. J. Coast. Res. 22, 209–223.

Klumpp, D.W., McKinnon, A.D., 1989. Temporal and spatial patterns in primary production of a coral-reef epilithic algal community. J. Exp. Mar. Biol. Ecol. 131, 1–22.

Kramer, M.J., Bellwood, D.R., Bellwood, O., 2012. Cryptofauna of the epilithic algal matrix on an inshore coral reef, Great Barrier Reef. Coral Reefs 31, 1007–1015.

Krone, R., Paster, M., Schuhmacher, H., 2011. Effect of the surgeonfish *Ctenochaetus striatus* (Acanthuridae) on the processes of sediment transport and deposition on a coral reef in the Red Sea. Facies 57, 215–221.

Lambrechts, J., Humphrey, C., McKinna, L., Gourge, O., Fabricius, K.E., Mehta, A.J., Lewis, S., Wolanski, E., 2010. Importance of wave-induced bed liquefaction in the fine sediment budget of Cleveland Bay, Great Barrier Reef. Estuar. Coast. Shelf Sci. 89, 154–162.

Larcombe, P., Woolfe, K.J., 1999. Increased sediment supply to the Great Barrier Reef will not increase sediment accumulation at most coral reefs. Coral Reefs 18, 163–169.

Larcombe, P., Ridd, P.V., Prytz, A., Wilson, B., 1995. Factors controlling suspended sediment on inner-shelf coral reefs, Townsville, Australia. Coral Reefs 14, 163–171.

Larcombe, P., Costen, A., Woolfe, K.J., 2001. The hydrodynamic and sedimentary setting of nearshore coral reefs, central Great Barrier Reef shelf, Australia: Paluma Shoals, a case study. Sedimentology 48, 811–835.

Latrille, F.X., Tebbett, S.B., Bellwood, D.R., 2019. Quantifying sediment dynamics on an inshore coral reef: putting algal turfs in perspective. Mar. Pollut. Bull. 141, 404–415.

Layton, C., Cameron, M.J., Shelamoff, V., Fernández, P.A., Britton, D., Hurd, C.L., Wright, J.T., Johnson, C.R., 2019. Chemical microenvironments within macroalgal assemblages: implications for the inhibition of kelp recruitment by turf algae. Limnol. Oceanogr. 64, 1600–1613.

Lenth, R., 2020. emmeans: Estimated Marginal Means, aka Least-Squares Means R package version 1.5.1.

Lewis, S.M., Wainwright, P.C., 1985. Herbivore abundance and grazing intensity on a Caribbean coral reef. J. Exp. Mar. Biol. Ecol. 81, 215–228.

Liao, Z., Yu, K., Wang, Y., Huang, X., Xu, L., 2019. Coral-algal interactions at Weizhou Island in the northern South China Sea: variations by taxa and the exacerbating impact of sediments trapped in turf algae. PeerJ 7, e6590.

Logan, D., Townsend, K.A., Townsend, K., Tibbetts, I.R., 2008. Meiofauna sediment relations in leeward slope turf algae of Heron Island reef. Hydrobiologia 610, 269–276.

Lutzenkirchen, L.L., Duce, S.J., Bellwood, D.R., 2023. The global biogeography of reef morphology. Glob. Ecol. Biogeogr. https://doi.org/10.1111/geb.13699.

Mallela, J., Roberts, C., Harrod, C., Goldspink, C.R., 2007. Distributional patterns and community structure of Caribbean coral reef fishes within a river-impacted bay. J. Fish Biol. 70, 523–537.

Margvelashvili, N., Andrewartha, J., Herzfeld, M., Robson, B.J., Brando, V.E., 2013. Satellite data assimilation and estimation of a 3D coastal sediment transport model using error-subspace emulators. Environ. Model. Softw. 40, 191–201.

McClure, E.C., Richardson, L.E., Graba-landry, A., Loffler, Z., Russ, G.R., Hoey, A.S., 2019. Cross-shelf differences in the response of herbivorous fish assemblages to severe environmental disturbances. Diversity 11, 23.

Miller, M.W., Karazsia, J., Groves, C.E., Griffin, S., Moore, T., Wilber, P., Gregg, K., 2016. Detecting sedimentation impacts to coral reefs resulting from dredging the Port of Miami, Florida, USA. PeerJ 4, e2711.

Morais, J., Morais, R., Tebbett, S.B., Bellwood, D.R., 2022. On the fate of dead coral colonies. Funct. Ecol. 36, 3148–3160.

Morgan, K.M., Kench, P.S., 2014. A detrital sediment budget of a Maldivian reef platform. Geomorphology 222, 122–131.

Morgan, K.M., Kench, P.S., 2016. Parrotfish erosion underpins reef growth, sand talus development and island building in the Maldives. Sediment. Geol. 341, 50–57.

Moustaka, M., Langlois, T.J., Mclean, D., Bond, T., Fisher, R., Fearns, P., Dorji, P., Evans, R.D., 2018. The effects of suspended sediment on coral reef fish assemblages and feeding guilds of north-west Australia. Coral Reefs 37, 659–673.

Moustaka, M., Mohring, M.B., Holmes, T., Evans, R.D., Thomson, D., Nutt, C., Stoddart, J., Wilson, S.K., 2019. Cross-shelf heterogeneity of coral assemblages in Northwest Australia. Diversity 11, 15.

Ng, D., Taira, D., Heery, E.C., Todd, P.A., 2021. Antagonistic effects of seawalls and urban sedimentation on epilithic algal matrix (EAM)-feeding fishes. Mar. Pollut. Bull. 173, 113098.

Ng, M.S., Teo, A., Todd, P.A., 2022. Sediment trap height affects mass, particle size, and biogeochemical composition of material collected in an equatorial coral reef. Mar. Pollut. Bull. 183, 114086.

O'Brien, J.M., Scheibling, R.E., 2018. Turf wars: competition between foundation and turf-forming species on temperate and tropical reefs and its role in regime shifts. Mar. Ecol. Prog. Ser. 590, 1–17.

Ogston, A.S., Storlazzi, C.D., Field, M.E., Presto, M.K., 2004. Sediment resuspension and transport patterns on a fringing reef flat, Molokai, Hawaii. Coral Reefs 23, 559–569.

Orpin, A.R., Ridd, P.V., Stewart, L.K., 1999. Assessment of the relative importance of major sediment transport mechanisms in the central Great Barrier Reef lagoon. Aust. J. Earth Sci. 46, 883–896.

Perry, C.T., Salter, M.A., Lange, I.D., Kochan, D.P., Harborne, A.R., Graham, N.A.J., 2022. Geo-ecological functions provided by coral reef fishes vary among regions and impact reef carbonate cycling regimes. Ecosphere 13, e4288.

Pessarrodona, A., Filbee-Dexter, K., Alcoverro, T., Boada, J., Feehan, C.J., Fredriksen, S., Grace, S.P., Nakamura, Y., Narvaez, C.A., Norderhaug, K.M., Wernberg, T., 2021. Homogenization and miniaturization of habitat structure in temperate marine forests. Glob. Chang. Biol. 27, 5262–5275.

Pessarrodona, A., Vergés, A., Bosch, N.E., Bell, S., Smith, S., Sgarlatta, M.P., Wernberg, T., 2022. Tropicalization unlocks novel trophic pathways and enhances secondary productivity in temperate reefs. Funct. Ecol. 36, 659–673.

Pomeroy, A.W.M., Lowe, R.J., Ghisalberti, M., Winter, G., Storlazzi, C., Cuttler, M., 2018. Spatial variability of sediment transport processes over intratidal and subtidal timescales within a fringing coral reef system. J. Geophys. Res. Earth Surf. 123, 1013–1034.

Pomeroy, A.W.M., Storlazzi, C.D., Rosenberger, K.J., Lowe, R.J., Hansen, J.E., Buckley, M.L., 2021. The contribution of currents, sea-swell waves, and infragravity waves to suspended-sediment transport across a coral reef-lagoon system. J. Geophys. Res. Oceans 126, e2020JC017010.

Prathep, A., Marrs, R.H., Norton, T.A., 2003. Spatial and temporal variations in sediment accumulation in an algal turf and their impact on associated fauna. Mar. Biol. 142, 381–390.

Purcell, S.W., 2000. Association of epilithic algae with sediment distribution on a windward reef in the northern Great Barrier Reef, Australia. Bull. Mar. Sci. 66, 199–214.

Purcell, S.W., Bellwood, D.R., 2001. Spatial patterns of epilithic algal and detrital resources on a windward coral reef. Coral Reefs 20, 117–125.

R Core Team, 2022. R: A Language and Environment for Statistical Computing. R Foundation for Statistical Computing, Vienna, Austria.

Reeves, S.E., Kriegisch, N., Johnson, C.R., Ling, S.D., 2018. Reduced resistance to sediment - trapping turfs with decline of native kelp and establishment of an exotic kelp. Oecologia 188, 1239–1251.

Ricardo, G.F., Harper, C.E., Negri, A.P., Luter, H.M., Abdul Wahab, M.A., Jones, R.J., 2021. Impacts of water quality on *Acropora* coral settlement: the relative importance of substrate quality and light. Sci. Total Environ. 777, 146079.

Roff, G., Bejarano, S., Priest, M., Marshell, A., Chollett, I., Steneck, R.S., Doropoulos, C., Golbuu, Y., Mumby, P.J., 2019. Seascapes as drivers of herbivore assemblages in coral reef ecosystems. Ecol. Monogr. 89, e01336.

Russ, G.R., 2003. Grazer biomass correlates more strongly with production than with biomass of algal turfs on a coral reef. Coral Reefs 22, 63–67.

Ryan, E.J., Smithers, S.G., Lewis, S.E., Clark, T.R., Zhao, J., 2018. The variable influences of sea level, sedimentation and exposure on holocene reef development over a cross-shelf transect, central Great Barrier Reef. Diversity 10, 110.

Samoilys, M.A., Halford, A., Osuka, K., 2019. Disentangling drivers of the abundance of coral reef fishes in the Western Indian Ocean. Ecol. Evol. 9, 4149–4167.

Santana, E.F.C., Mies, M., Longo, G.O., Menezes, R., Aued, A.W., Luza, A.L., Bender, M.G., Segal, B., Floeter, S.R., Francini-Filho, R.B., 2023. Turbidity shapes shallow Southwestern Atlantic benthic reef communities. Mar. Environ. Res. 183, 105807.

Schaffelke, B., Thompson, A., Carleton, J., Davidson, J., Doyle, J., Furnas, M., Gunn, K., Skuza, M., Wright, M., Zagorskis, I., 2009. Reef Rescue Marine Monitoring Program. Final Report of AIMS Activities 2008/09. Australian Institute of Marine Science, Townsville, Australia.

Schlaefer, J.A., Tebbett, S.B., Bellwood, D.R., 2021. The study of sediments on coral reefs: a hydrodynamic perspective. Mar. Pollut. Bull. 169, 112580.

Schlaefer, J.A., Tebbett, S.B., Bowden, C.L., Collins, W.P., Duce, S., Hemingson, C.R., Huertas, V., Mihalitsis, M., Morais, J., Morais, R.A., Siqueira, A.C., Streit, R.P., Swan, S., Valenzuela, J., Bellwood, D.R., 2022. A snapshot of sediment dynamics on an inshore coral reef. Mar. Environ. Res. 181, 105763.

Seabold, S., Perktold, J., 2010. Statsmodels: Econometric and Statistical Modeling With Python.

Siqueira, A.C., Morais, R.A., Bellwood, D.R., Cowman, P.F., 2020. Trophic innovations fuel reef fish diversification. Nat. Commun. 11, 2669.

Smith, J.E., Brainard, R., Carter, A., Grillo, S., Edwards, C., Harris, J., Lewis, L., Obura, D., Rohwer, F., Sala, E., Vroom, P.S., Sandin, S., 2016. Re-evaluating the health of coral reef communities: baselines and evidence for human impacts across the central Pacific. Proc. R. Soc. B Biol. Sci. 283, 20151985.

Soulsby, R.L., Hamm, L., Klopman, G., Myrhaug, D., Simons, R.R., Thomas, G.P., 1993. Wave-current interaction within and outside the bottom boundary layer. Coast. Eng. 21, 41–69.

Speare, K.E., Duran, A., Miller, M.W., Burkepile, D.E., 2019. Sediment associated with algal turfs inhibits the settlement of two endangered coral species. Mar. Pollut. Bull. 144, 189–195.

Steneck, R.S., 1997. Crustose corallines, other algal functional groups, herbivores and sediments: complex interactions along reef productivity gradients. Proceedings of the 8th International Coral Reef Symposium. 1, pp. 695–700.

Stoddart, D.R., 1969. Ecology and morphology of recent coral reefs. Biol. Rev. 44, 433–498.

Storlazzi, C.D., Jaffe, B.E., 2008. The relative contribution of processes driving variability in flow, shear, and turbidity over a fringing coral reef: West Maui, Hawaii. Estuar. Coast. Shelf Sci. 77, 549–564.

Storlazzi, C.D., Ogston, A.S., Bothner, M.H., Field, M.E., Presto, M.K., 2004. Wave- and tidally-driven flow and sediment flux across a fringing coral reef: Southern Molokai, Hawaii. Cont. Shelf Res. 24, 1397–1419.

Storlazzi, C.D., Field, M.E., Bothner, M.H., Presto, M.K., Draut, A.E., 2009. Sedimentation processes in a coral reef embayment: Hanalei Bay, Kauai. Mar. Geol. 264, 140–151.

Storlazzi, C.D., Field, M.E., Bothner, M.H., 2011. The use (and misuse) of sediment traps in coral reef environments: theory, observations, and suggested protocols. Coral Reefs 30, 23–38.

Suárez-Castro, A.F., Beyer, H.L., Kuempel, C.D., Linke, S., Borrelli, P., Hoegh-Guldberg, O., 2021. Global forest restoration opportunities to foster coral reef conservation. Glob. Chang. Biol. 27, 5238–5252.

Taylor, B.M., Brandl, S.J., Kapur, M., Robbins, W.D., Johnson, G., Huveneers, C., Renaud, P., Choat, J.H., 2018. Bottom-up processes mediated by social systems drive demographic traits of coral-reef fishes. Ecology 99, 642–651.

Tebbett, S.B., Bellwood, D.R., 2020. Sediments ratchet-down coral reef algal turf productivity. Sci. Total Environ. 713, 136709.

Tebbett, S.B., Goatley, C.H.R., Bellwood, D.R., 2017a. Algal turf sediments and sediment production by parrotfishes across the continental shelf of the northern Great Barrier Reef. PLoS One 12, e0170854.

Tebbett, S.B., Goatley, C.H.R., Bellwood, D.R., 2017b. Fine sediments suppress detritivory on coral reefs. Mar. Pollut. Bull. 114, 934–940.

Tebbett, S.B., Bellwood, D.R., Purcell, S.W., 2018. Sediment addition drives declines in algal turf yield to herbivorous coral reef fishes: implications for reefs and reef fisheries. Coral Reefs 37, 929–937.

Tebbett, S.B., Goatley, C.H.R., Streit, R.P., Bellwood, D.R., 2020. Algal turf sediments limit the spatial extent of function delivery on coral reefs. Sci. Total Environ. 734, 139422.

Tebbett, S.B., Morais, R.A., Goatley, C.H.R., Bellwood, D.R., 2021. Collapsing ecosystem functions on an inshore coral reef. J. Environ. Manag. 289, 112471.

Tebbett, S.B., Morais, J., Bellwood, D.R., 2022a. Spatial patchiness in change, recruitment, and recovery on coral reefs at Lizard Island following consecutive bleaching events. Mar. Environ. Res. 173, 105537.

Tebbett, S.B., Sgarlatta, M.P., Pessarrodona, A., Vergés, A., Wernberg, T., Bellwood, D.R., 2022b. How to quantify algal turf sediments and particulates on tropical and temperate reefs: an overview. Mar. Environ. Res. 179, 105673.

Tebbett, S.B., Siqueira, A.C., Bellwood, D.R., 2022c. The functional roles of surgeonfishes on coral reefs: past, present and future. Rev. Fish Biol. Fish. 32, 387–439.

Tebbett, S.B., Streit, R.P., Morais, J., Schlaefer, J.A., Swan, S., Bellwood, D.R., 2022d. Benthic cyanobacterial mat formation during severe coral bleaching at Lizard Island: the mediating role of water currents. Mar. Environ. Res. 181, 105752.

Tebbett, S.B., Connolly, S.R., Bellwood, D.R., 2023a. Benthic composition changes on coral reefs at global scales. Nat. Ecol. Evol. 7, 71–81.

Tebbett, S.B., Crisp, S.K., Evans, R.D., Fulton, C.J., Pessarrodona, A., Wernberg, T., Wilson, S.K., Bellwood, D.R., 2023b. On the challenges of identifying benthic dominance on Anthropocene coral reefs. BioScience 73, 220–228.

Thomson, D.P., Babcock, R.C., Evans, R.D., Feng, M., Moustaka, M., Orr, M., Slawinski, D., Wilson, S.K., Hoey, A.S., 2021. Coral larval recruitment in north-western Australia predicted by regional and local conditions. Mar. Environ. Res. 168, 105318.

Victor, S., Neth, L., Golbuu, Y., Wolanski, E., Richmond, R.H., 2006. Sedimentation in mangroves and coral reefs in a wet tropical island, Pohnpei, Micronesia. Estuar. Coast. Shelf Sci. 66, 409–416.

Watanabe, H., Ito, M., Matsumoto, A., Arakawa, H., 2016. Effects of sediment influx on the settlement and survival of canopy-forming macrophytes. Sci. Rep. 6, 18677.

Weeks, S., Werdell, P.J., Schaffelke, B., Canto, M., Lee, Z., Wilding, J.G., Feldman, G.C., 2012. Satellite-derived photic depth on the Great Barrier Reef: spatio-temporal patterns of water clarity. Remote Sens. 4, 3781–3795.

Whinney, J., Jones, R., Duckworth, A., Ridd, P., 2017. Continuous in situ monitoring of sediment deposition in shallow benthic environments. Coral Reefs 36, 521–533.

Wolanski, E., Richmond, R.H., Davis, G., Bonito, V., 2003. Water and fine sediment dynamics in transient river plumes in a small, reef-fringed bay, Guam. Estuar. Coast. Shelf Sci. 56, 1029–1040.

Wolanski, E., Fabricius, K., Spagnol, S., Brinkman, R., 2005. Fine sediment budget on an inner-shelf coral-fringed island, Great Barrier Reef of Australia. Estuar. Coast. Shelf Sci. 65, 153–158.

Wolanski, E., Fabricius, K.E., Cooper, T.F., Humphrey, C., 2008. Wet season fine sediment dynamics on the inner shelf of the Great Barrier Reef. Estuar. Coast. Shelf Sci. 77, 755–762.

Wolanski, E., Martinez, J.A., Richmond, R.H., 2009. Quantifying the impact of watershed urbanization on a coral reef: Maunalua Bay, Hawaii. Estuar. Coast. Shelf Sci. 84, 259–268.

Yarlett, R.T., Perry, C.T., Wilson, R.W., Philpot, K.E., 2018. Constraining species-size class variability in rates of parrotfish bioerosion on Maldivian coral reefs: implications for regional-scale bioerosion estimates. Mar. Ecol. Prog. Ser. 590, 155–169.